

Quantum simulations with trapped ions

 universität
innsbruck

Institut für
Experimentalphysik

TIFR-ICTR online school, 18.5.2021

 ÖAW
ÖSTERREICHISCHE
AKADEMIE DER
WISSENSCHAFTEN

Funding:



FWF

Christian Roos
Institute for Experimental Physics
University of Innsbruck, Austria

Outline

- Quantum simulation approaches
 - Digital gate-based simulations
 - Crystal geometries
 - Analog simulations: engineering of long-range spin models
 - Detection and characterization of entangled states
- Variational quantum simulation
- Scaling quantum simulations to larger particle numbers

Simulating quantum physics

If there are quantum algorithms that run exponentially faster than their classical counterparts:

What stops us from simulating a quantum computer on a classical computer to find a solution in a much shorter time than with the classical algorithm?

Obstacle: There is no solution for simulating general quantum dynamics efficiently on a classical computer.



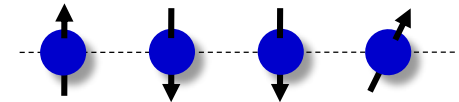
Maybe we should use a quantum processor to simulate the physics of quantum systems which is hard to simulate on classical computers

Quantum simulation

Quantum simulations with trapped ions

Simulating quantum many-body systems

How can we study the physics of quantum many-body systems?



Approaches:

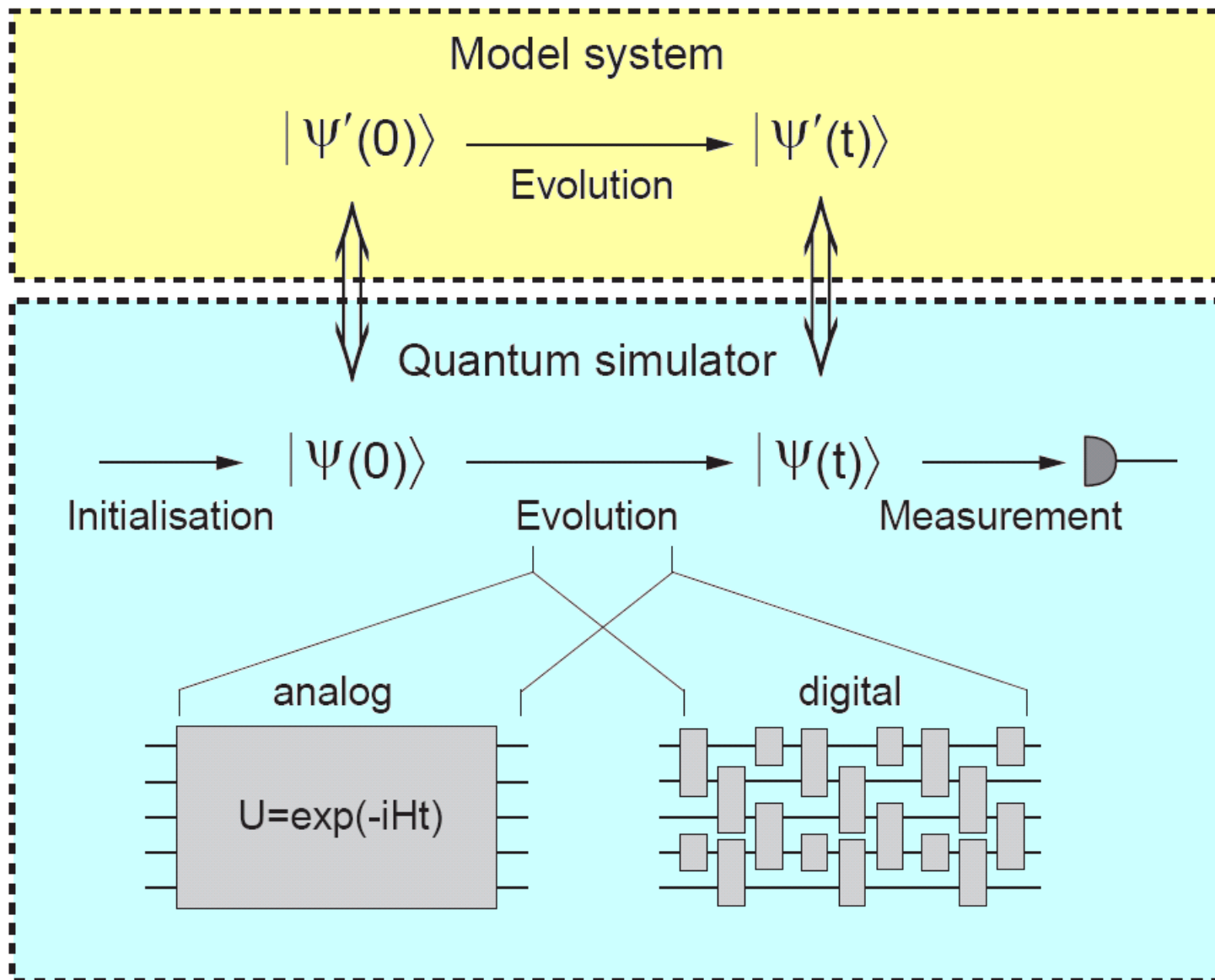
- In some cases: Analytical techniques
- Numerical simulation methods on a computer using approximations

But: Exponential scaling of resources with the system size severely restricts the number of particles that can be exactly simulated.

Interacting spins: exact diagonalization techniques limited to $N \sim 40$ spins

- Feynman (1982), Lloyd (1996): **Quantum simulators**
Use a precisely controlled quantum system for simulating a model of interest

Quantum simulation principle

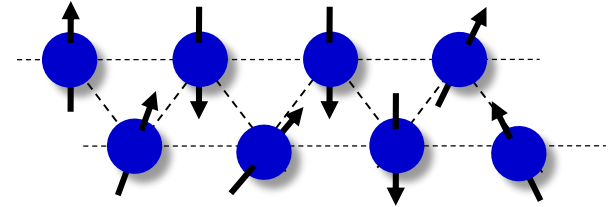


Simulating quantum spin systems

Hamiltonians:

- Ising model (with transverse field)

$$H = \frac{1}{2} \sum_{i,j} J_{ij} \sigma_i^x \sigma_j^x + B \sum_i \sigma_i^z$$



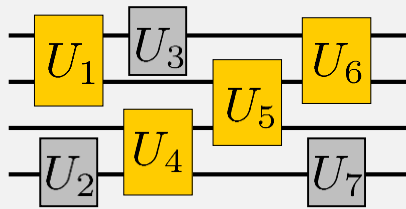
- XY model

$$H = \frac{1}{2} \sum_{i,j} J_{ij}^x \sigma_i^x \sigma_j^x + \frac{1}{2} \sum_{i,j} J_{ij}^y \sigma_i^y \sigma_j^y + B \sum_i \sigma_i^z$$

- Heisenberg model

$$H = \frac{1}{2} \sum_{i,j} J_{ij}^x \sigma_i^x \sigma_j^x + \frac{1}{2} \sum_{i,j} J_{ij}^y \sigma_i^y \sigma_j^y + \frac{1}{2} \sum_{i,j} J_{ij}^z \sigma_i^z \sigma_j^z + B \sum_i \sigma_i^z$$

Trapped-ion quantum simulations: Gate-based approach



Decompose dynamics induced by system Hamiltonian into sequence of quantum gates

$$U_{\text{sim}} \propto U_{\text{sys}}$$

$$U_{\text{sys}} = e^{-\frac{i}{\hbar} H_{\text{sys}} \tau}$$

Quantum gate toolbox:

- Single qubit-gates
- Entangling two-qubit gates

Building up Hamiltonians

Spin-spin interaction

$$H_{xx} = J \sigma_x^{(1)} \sigma_x^{(2)}$$

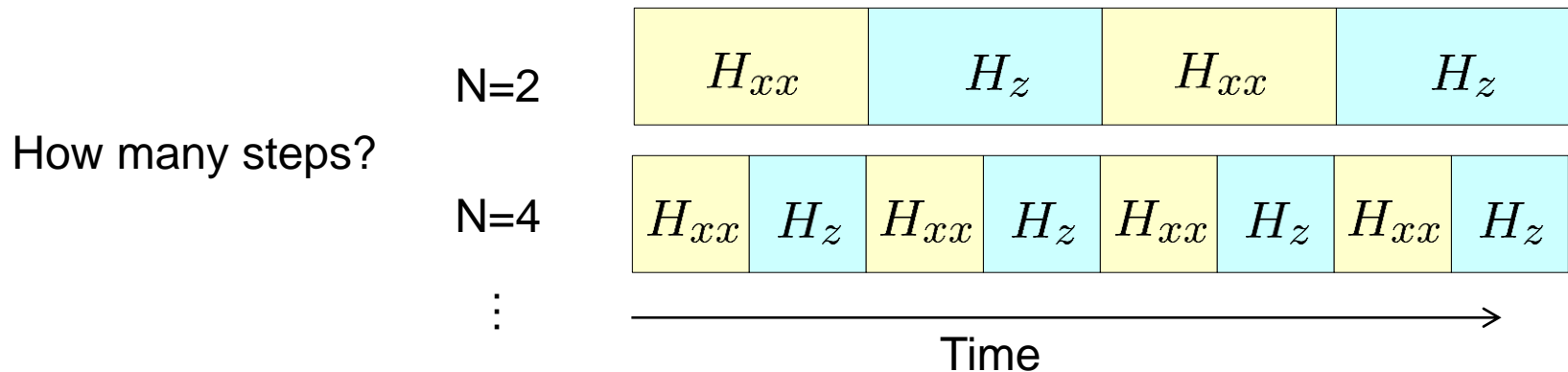
Can we add a transverse field? No... it would perturb the effective Hamiltonian H_{xx}

$$H = J \sigma_x^{(1)} \sigma_x^{(2)} + H_z$$

$$H_z = B (\sigma_z^{(1)} + \sigma_z^{(2)})$$

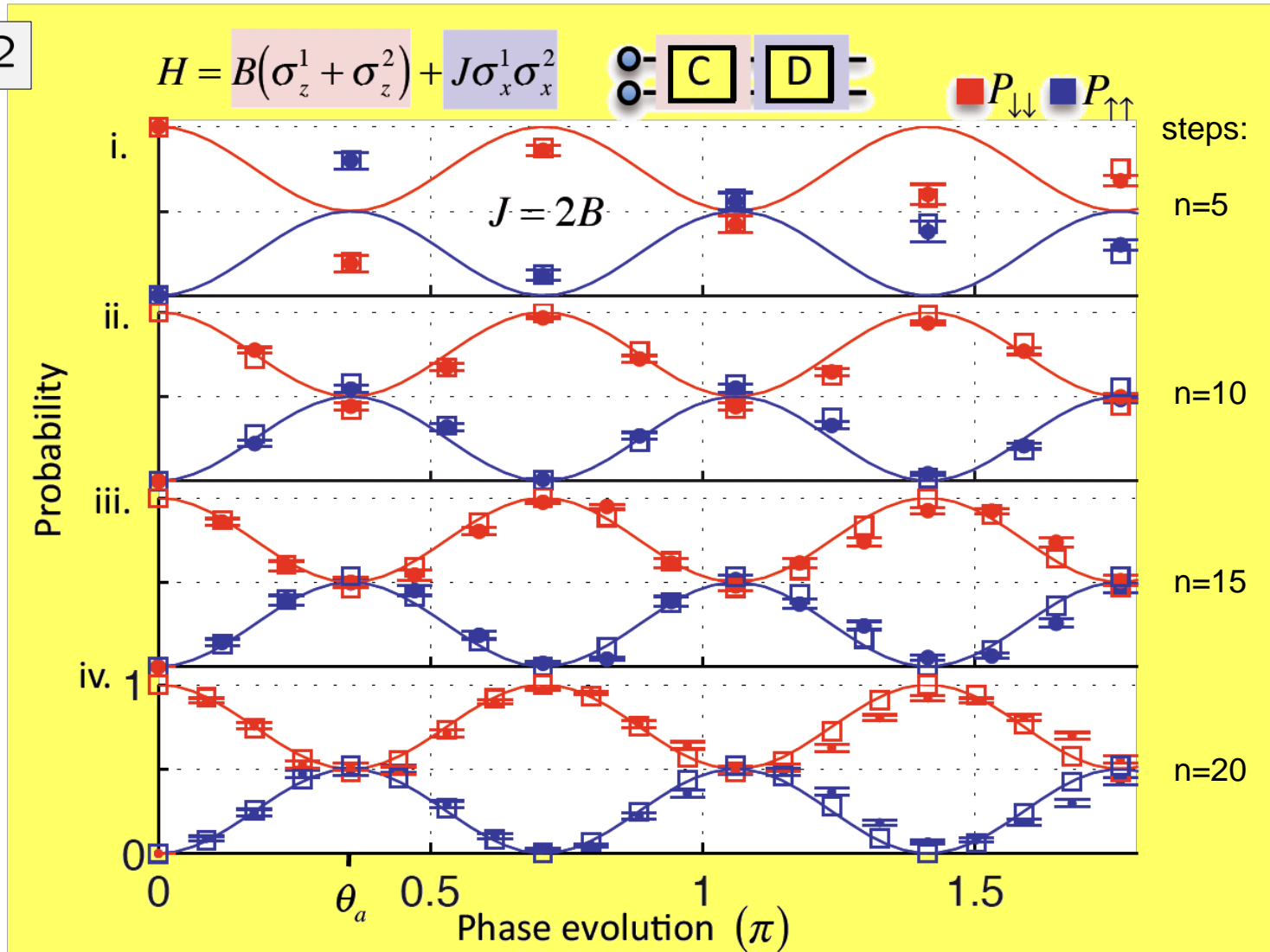
Solution: use 'Trotterization' to generate the dynamics corresponding to $H_{xx} + H_z$

$$U = e^{-i(H_{xx} + H_z)t} \approx e^{-iH_{xx}\Delta t} e^{-iH_z\Delta t} \dots e^{-iH_{xx}\Delta t} e^{-iH_z\Delta t}$$



Experimental 'Trotterization' of $H_{xx} + H_z$

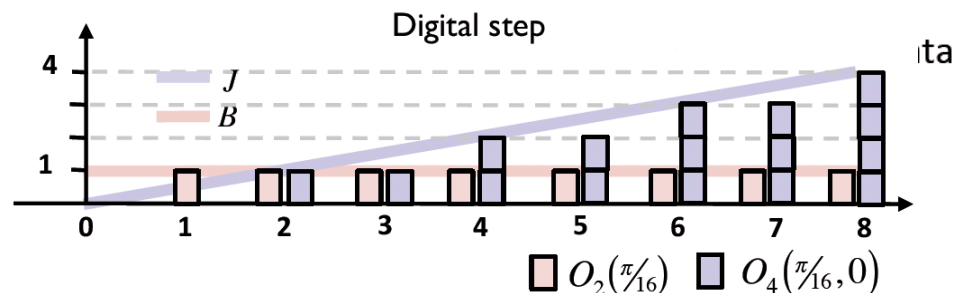
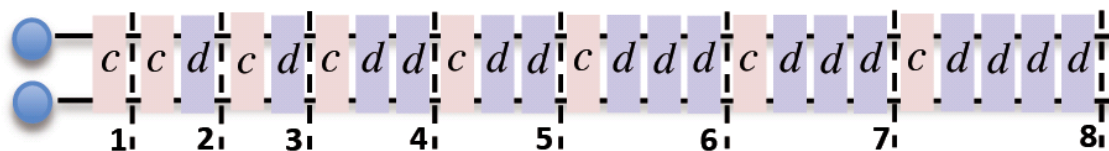
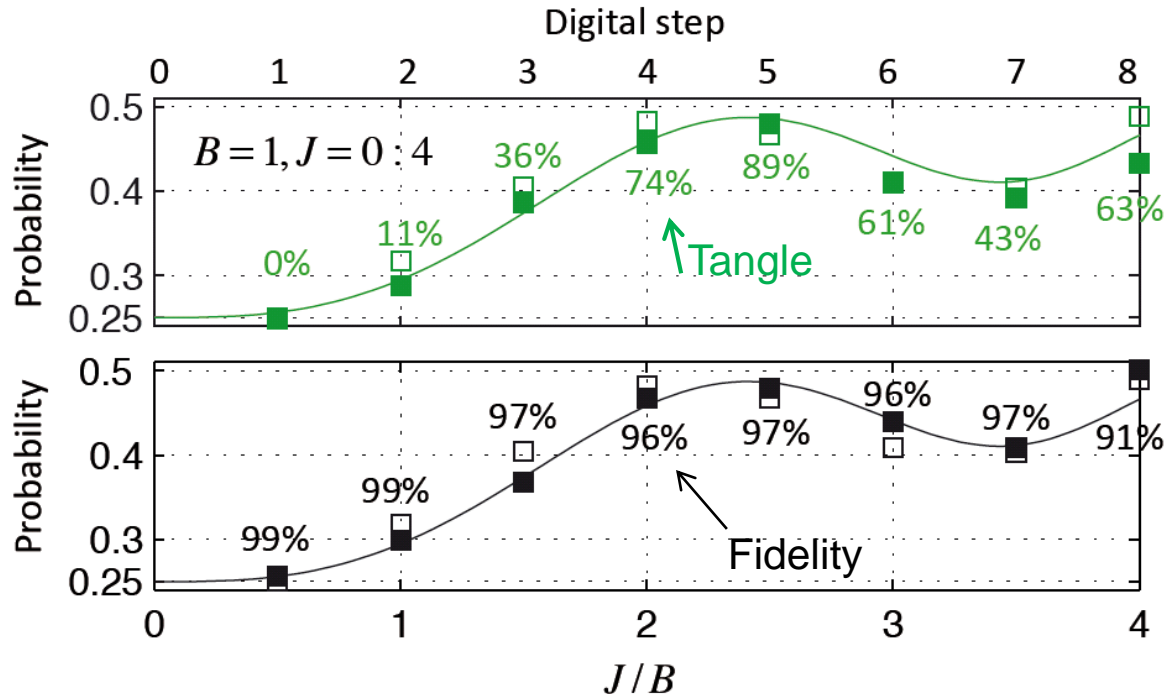
$$J/B = 2$$



Trotterization of (non-)adiabatic evolution

$$H = B(\sigma_z^1 + \sigma_z^2) + J\sigma_x^1\sigma_x^2$$

$$J/B = 0 \rightarrow 4$$

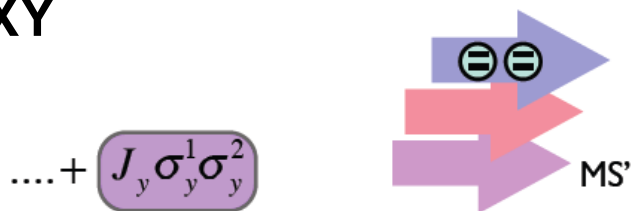


Building new interactions by Trotter technique

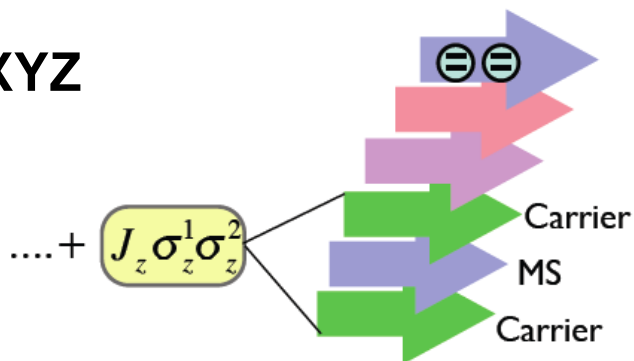
Ising



XY

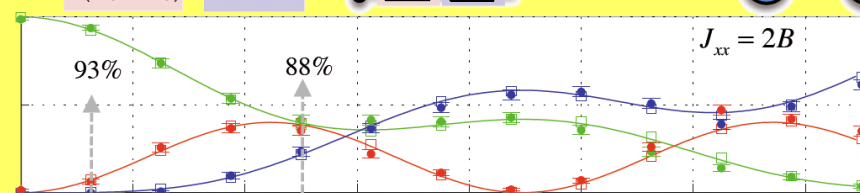


XYZ



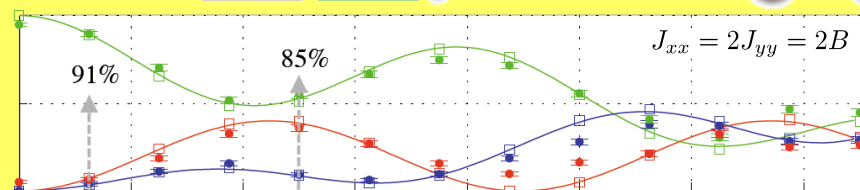
A Ising

$$H = B(\sigma_z^1 + \sigma_z^2) + J_{xx} \sigma_x^1 \sigma_x^2$$



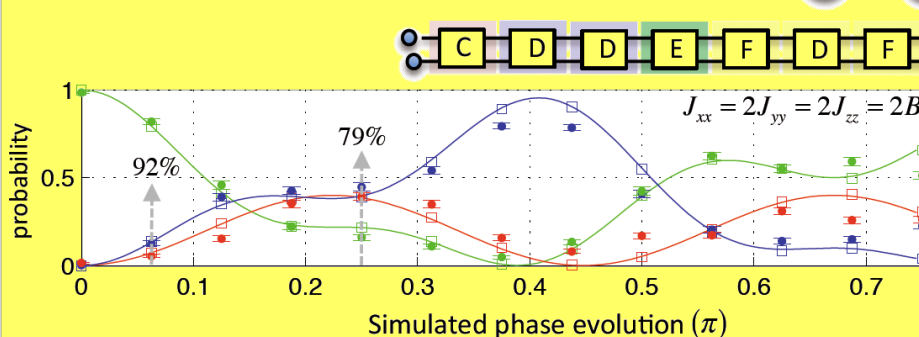
B XY

$$H = B(\sigma_z^1 + \sigma_z^2) + J_{xx} \sigma_x^1 \sigma_x^2 + J_{yy} \sigma_y^1 \sigma_y^2$$



C XYZ

$$H = B(\sigma_z^1 + \sigma_z^2) + J_{xx} \sigma_x^1 \sigma_x^2 + J_{yy} \sigma_y^1 \sigma_y^2 + J_{zz} \sigma_z^1 \sigma_z^2$$



— Exact
 □ Digitized
 ● Data

$$C = O_2(\pi/32)$$

$$D = O_4(\pi/16,0)$$

$$E = O_4(\pi/16,\pi)$$

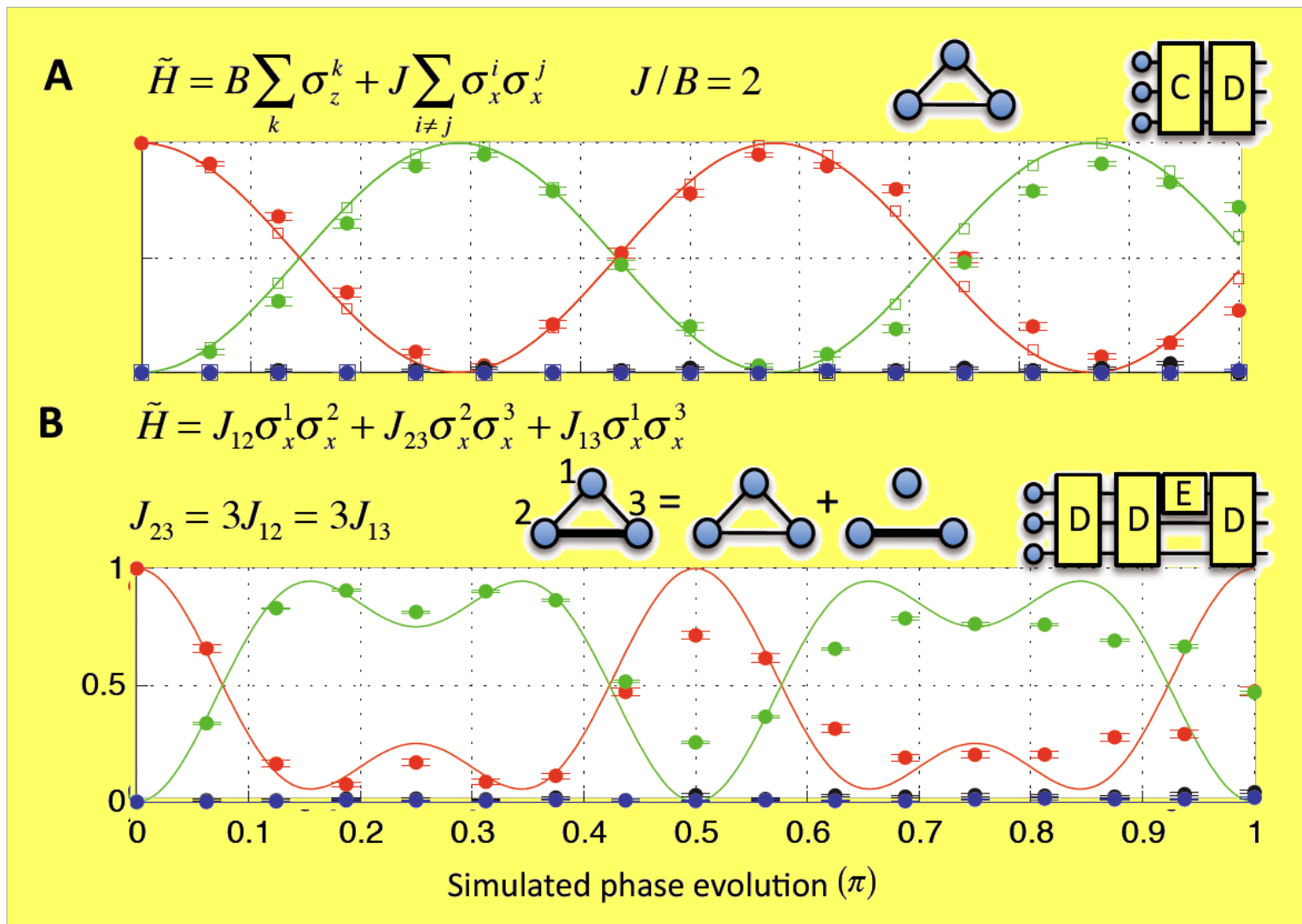
$$F = O_3(\pi/4,0)$$

$$P(\rightarrow, \leftarrow)$$

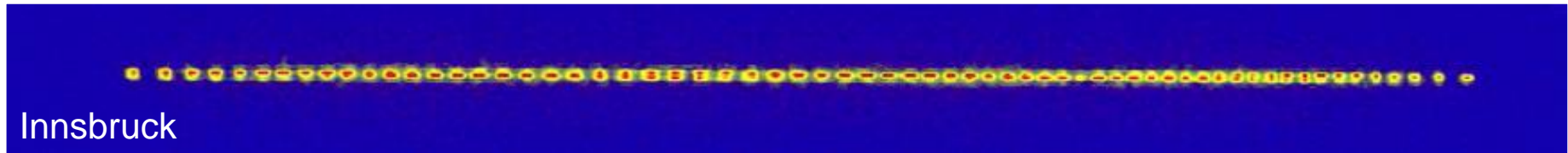
$$P(\leftarrow, \rightarrow)$$

$$P(\rightarrow, \rightarrow) + P(\leftarrow, \leftarrow)$$

Increasing the number of spins

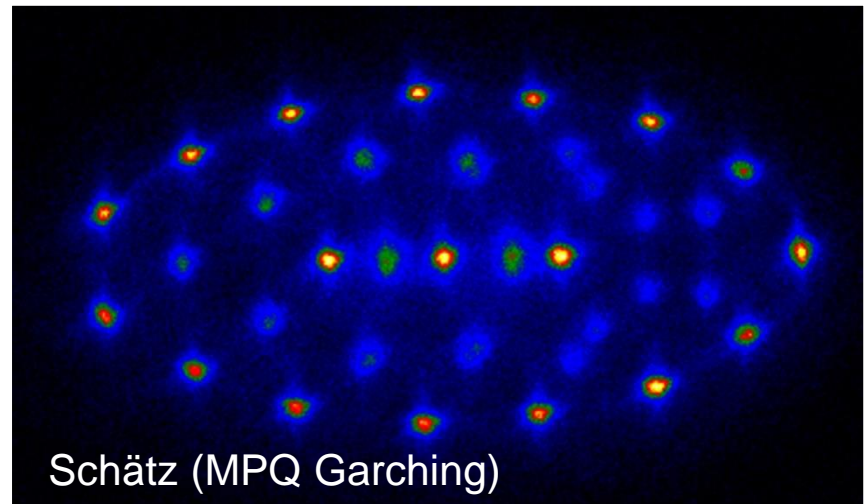
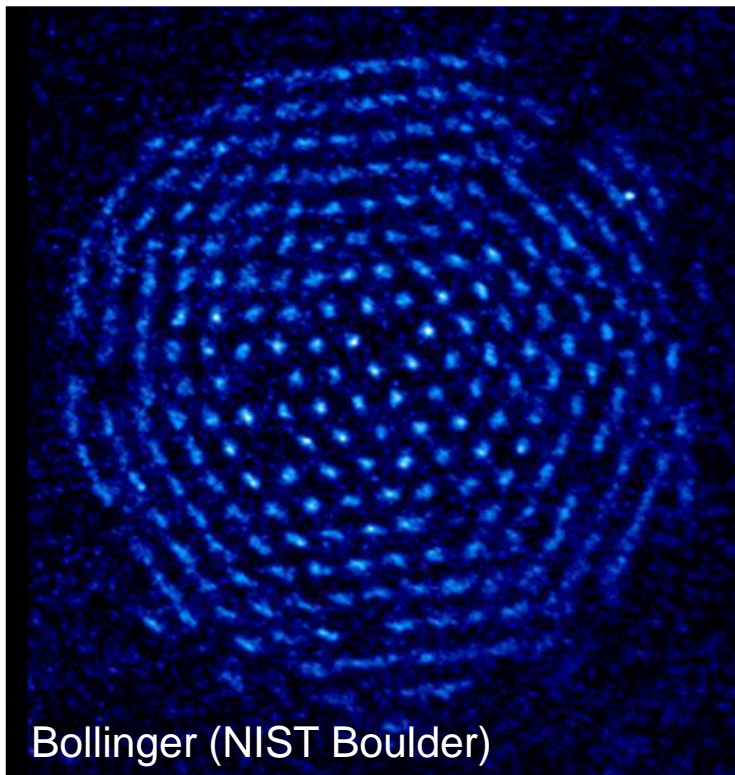


Trapped ions for simulating quantum magnetism



Challenges:

- Controlling the geometry
- Keeping decoherence low
- Engineering interactions



Trapping geometries: rf traps

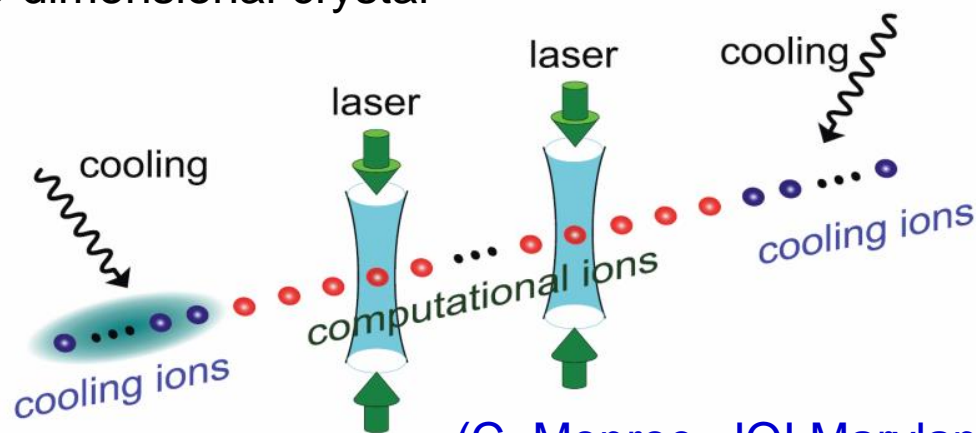
Linear traps: Harmonic anisotropic potentials

$N = 2 \dots 100(?)$ ions in a one-dimensional crystal

$$\frac{\omega_r}{\omega_z} > 0.77 \frac{N}{\log N} \quad \text{longer crystals require very anisotropic potentials}$$

Segmented microtraps: Anharmonic potentials for linear ion strings with equal spacing

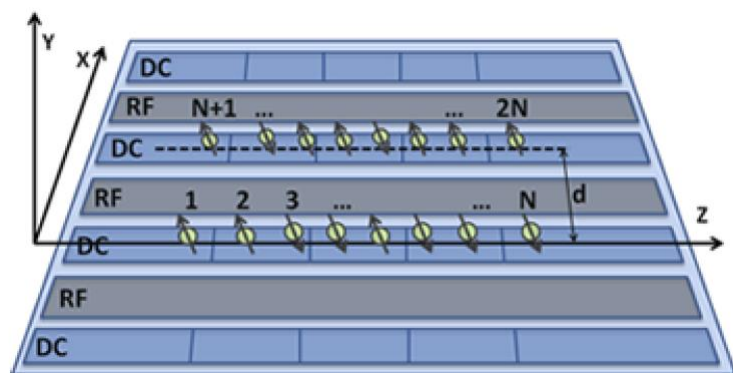
$N > 100(?)$ ions in a one-dimensional crystal



(C. Monroe, JQI Maryland)

Trapping geometries: rf traps

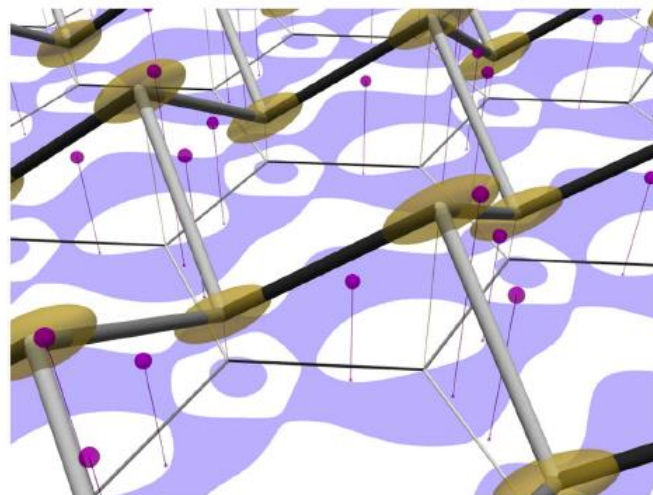
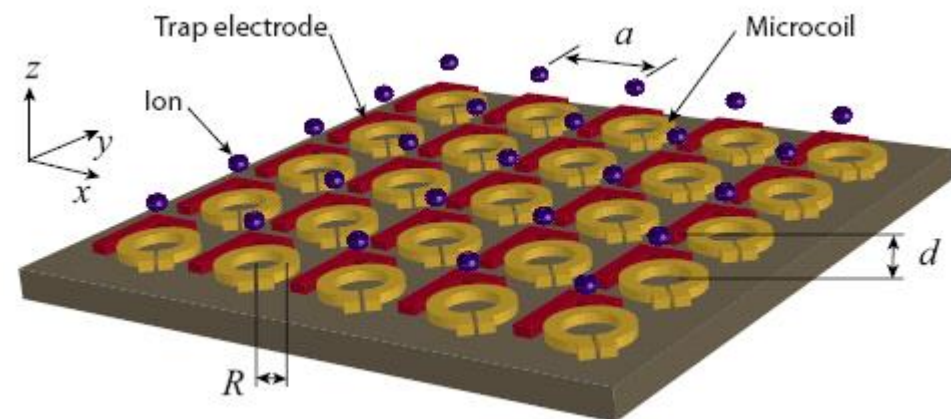
Segmented microtraps for Potentials with multipole trapping sites



Multiple linear strings in close proximity

J. Welzel et al., EPJD **65**, 285 (2011)

2d-lattices of trapping sites



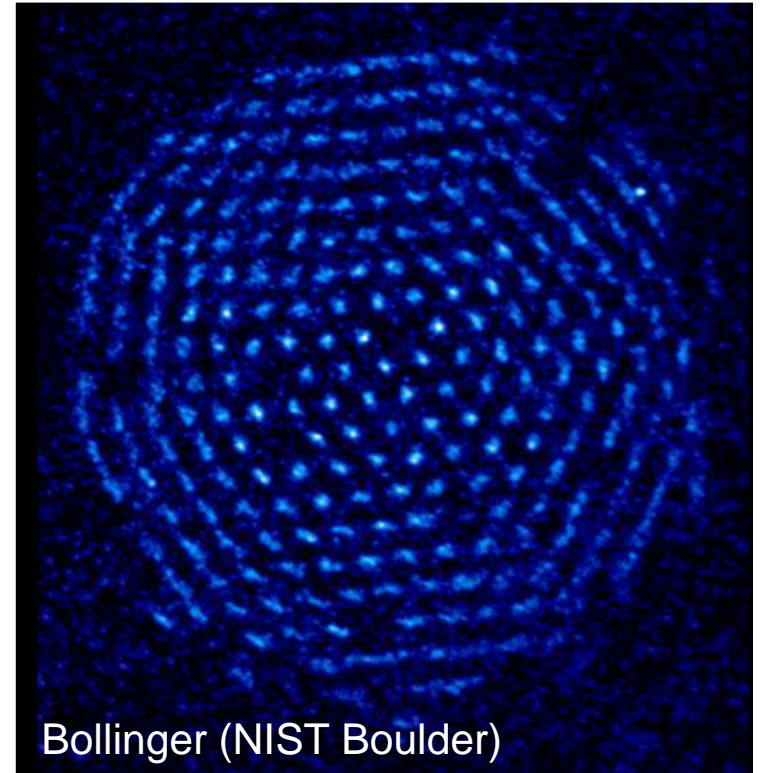
Chiaverini and Lybarger, *Phys. Rev. A* **77**, 022324 (2008)

R Schmied et al, *PRL* **102**, 233002 (2009)

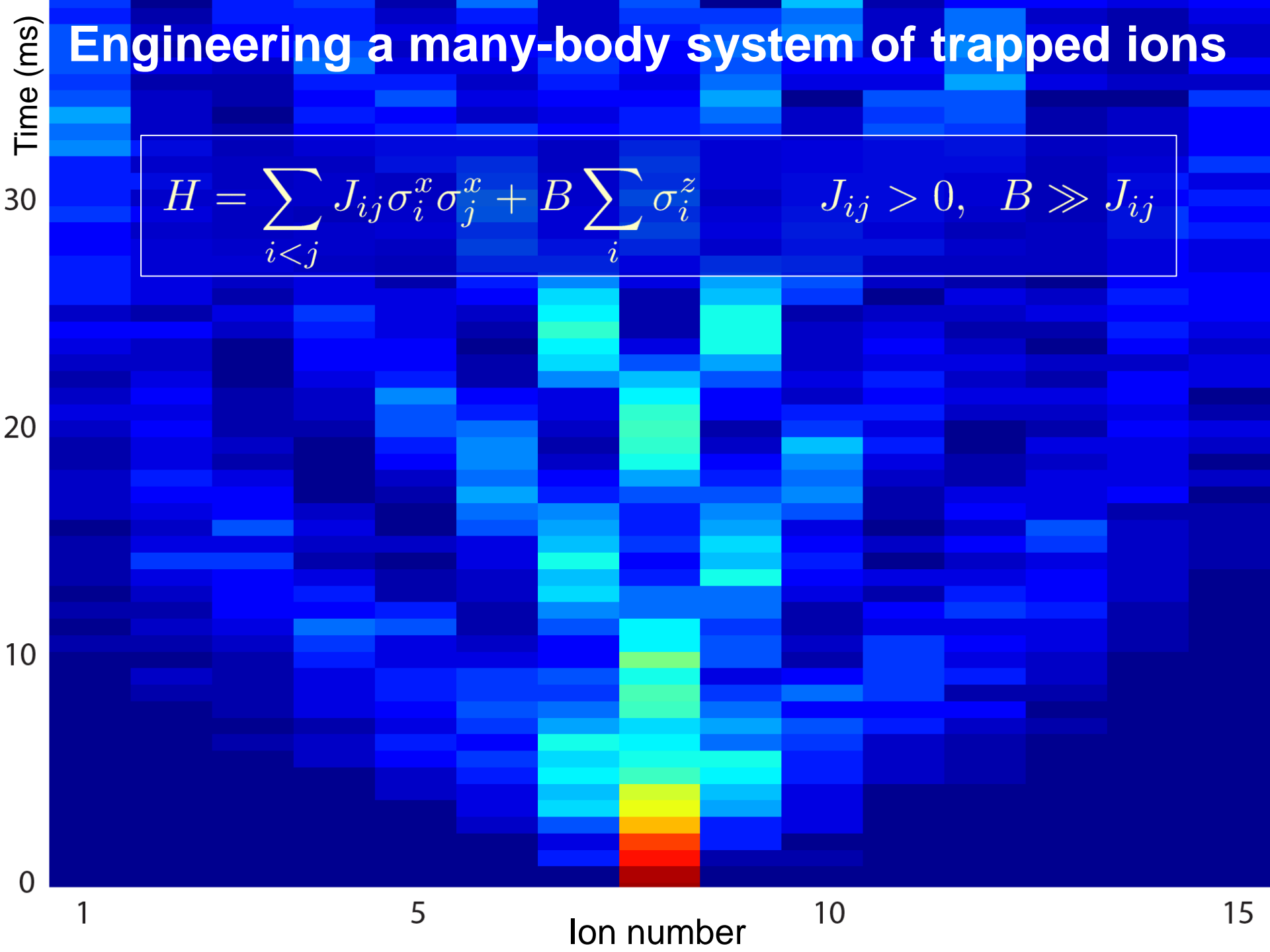
Trapping geometries: Penning traps

Penning trap: anisotropic potential for trapping 2d crystals

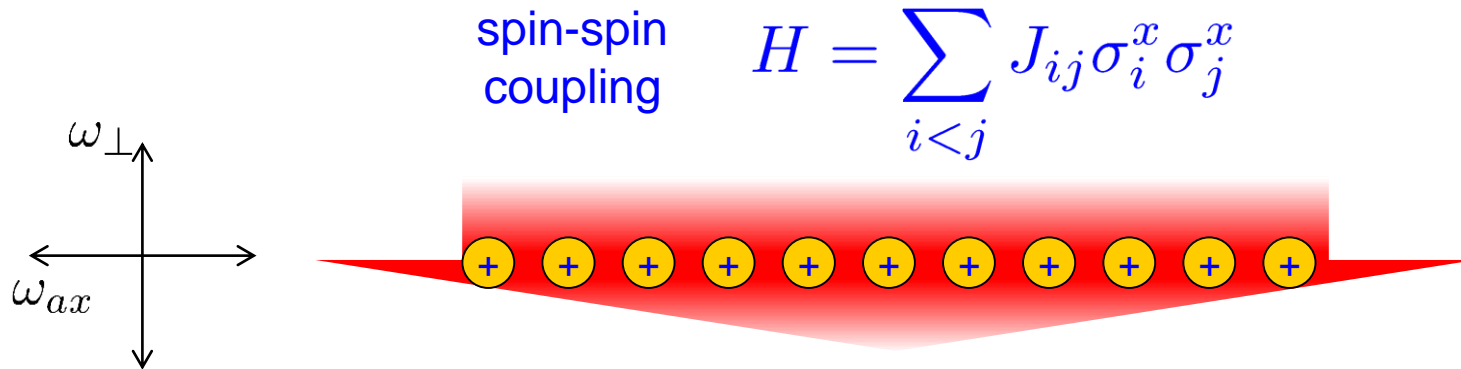
- $N \approx 100 - 300$ ions possible
- low internal state decoherence
- challenge: demonstrate same kind of quantum control as in rf-traps



Engineering a many-body system of trapped ions



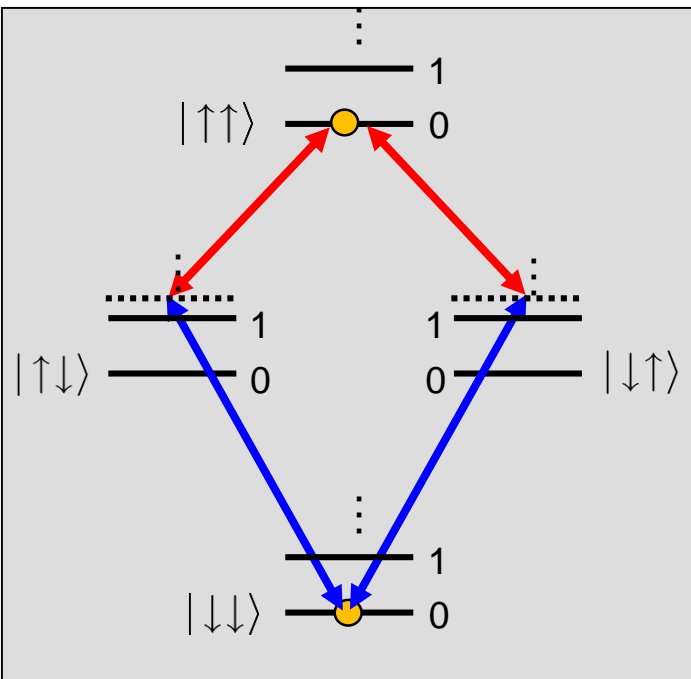
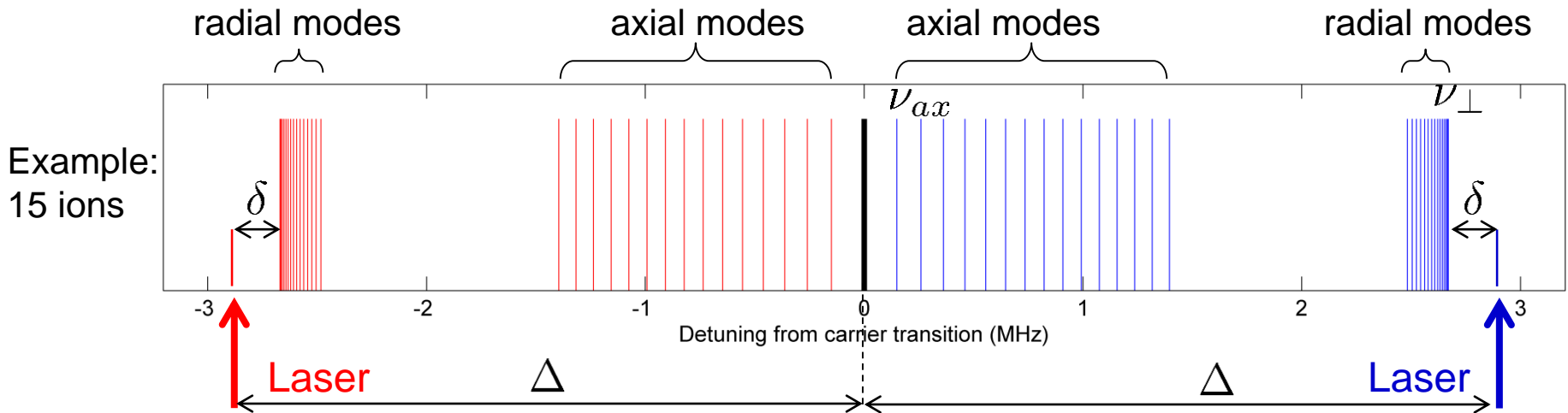
Geometry of laser-ion interaction



Features:

- Long strings \Rightarrow strongly anisotropic trapping potentials: $\omega_{\perp}/\omega_{ax} \approx 15 - 20$
- weak axial confinement \Rightarrow 'hot' axial modes \Rightarrow all laser beams \perp to ion string

Variable-range interactions by coupling to transverse modes



$$H = \sum_{i < j} J_{ij} \sigma_i^x \sigma_j^x$$

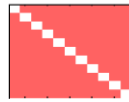
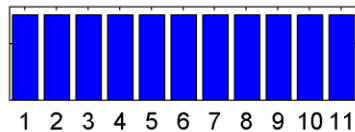
with

$$J_{ij} = \Omega^2 \frac{(\hbar k)^2}{2m} \sum_m \frac{b_{i,m} b_{j,m}}{\Delta^2 - \nu_m^2}$$

Variable-range interactions by coupling to transverse modes

Example: 11 ions

vibrational mode



'COM'

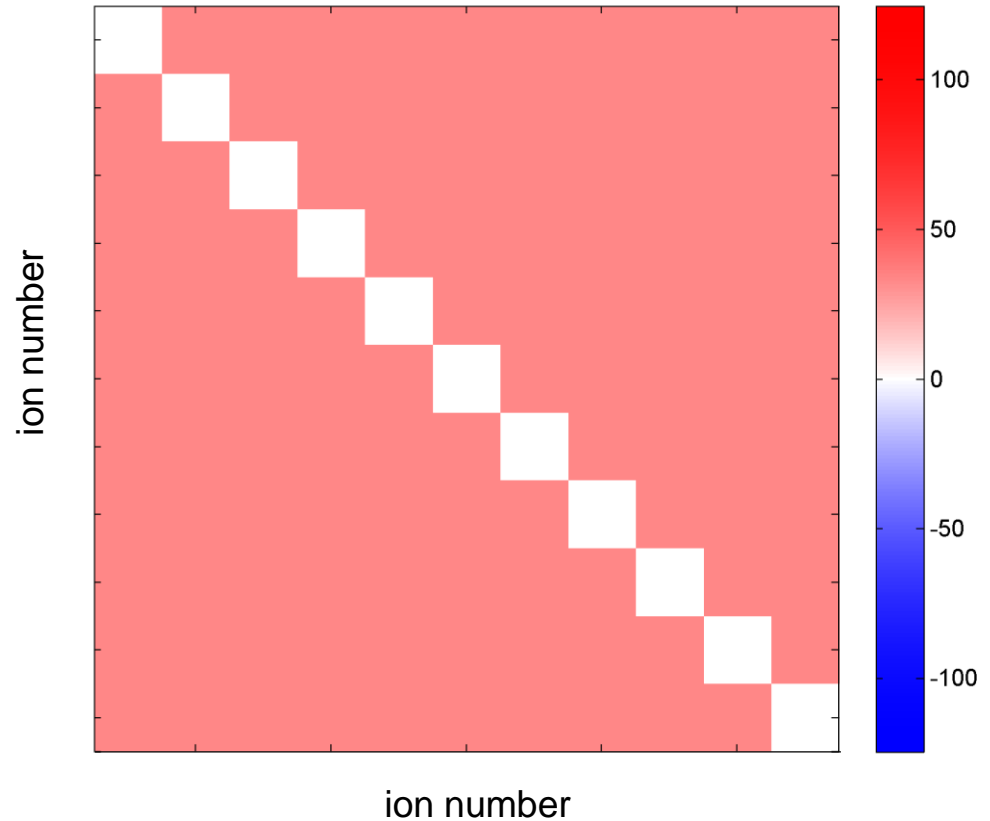
'Tilt'

⋮

⋮

$$J_{ij} = \Omega^2 \frac{(\hbar k)^2}{2m} \sum_m \frac{b_{i,m} b_{j,m}}{\Delta^2 - \nu_m^2}$$

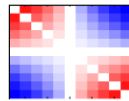
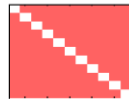
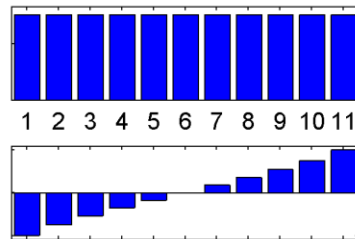
Spin-spin coupling matrix J_{ij} (Hz)



Variable-range interactions by coupling to transverse modes

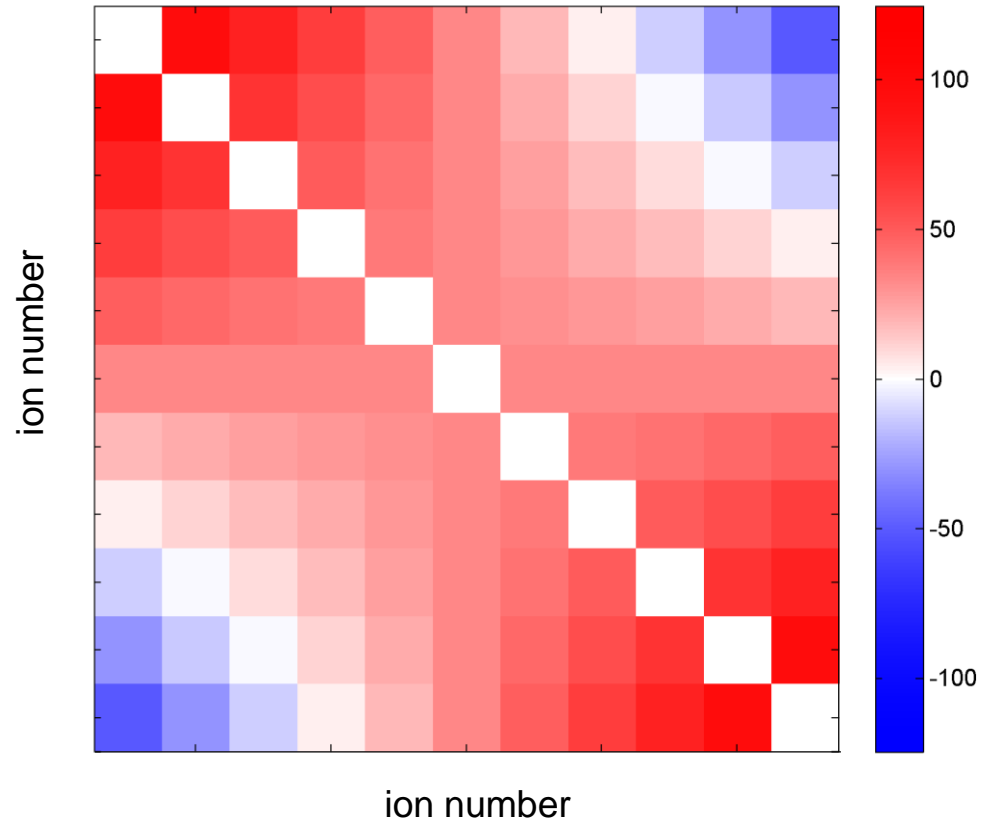
Example: 11 ions

vibrational mode



$$J_{ij} = \Omega^2 \frac{(\hbar k)^2}{2m} \sum_m \frac{b_{i,m} b_{j,m}}{\Delta^2 - \nu_m^2}$$

Spin-spin coupling matrix J_{ij} (Hz)

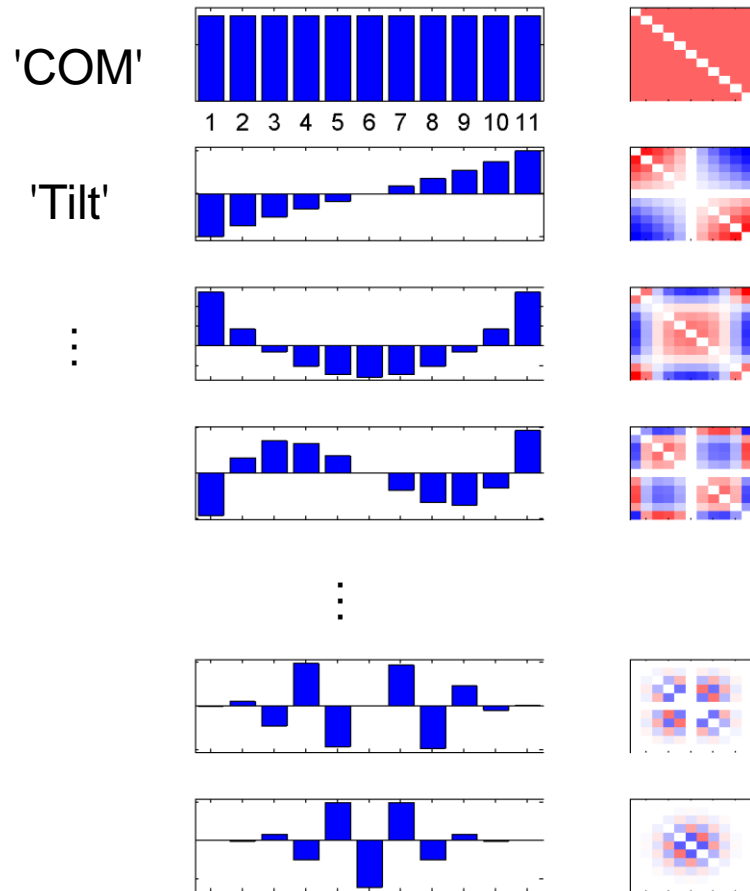


Variable-range interactions by coupling to transverse modes

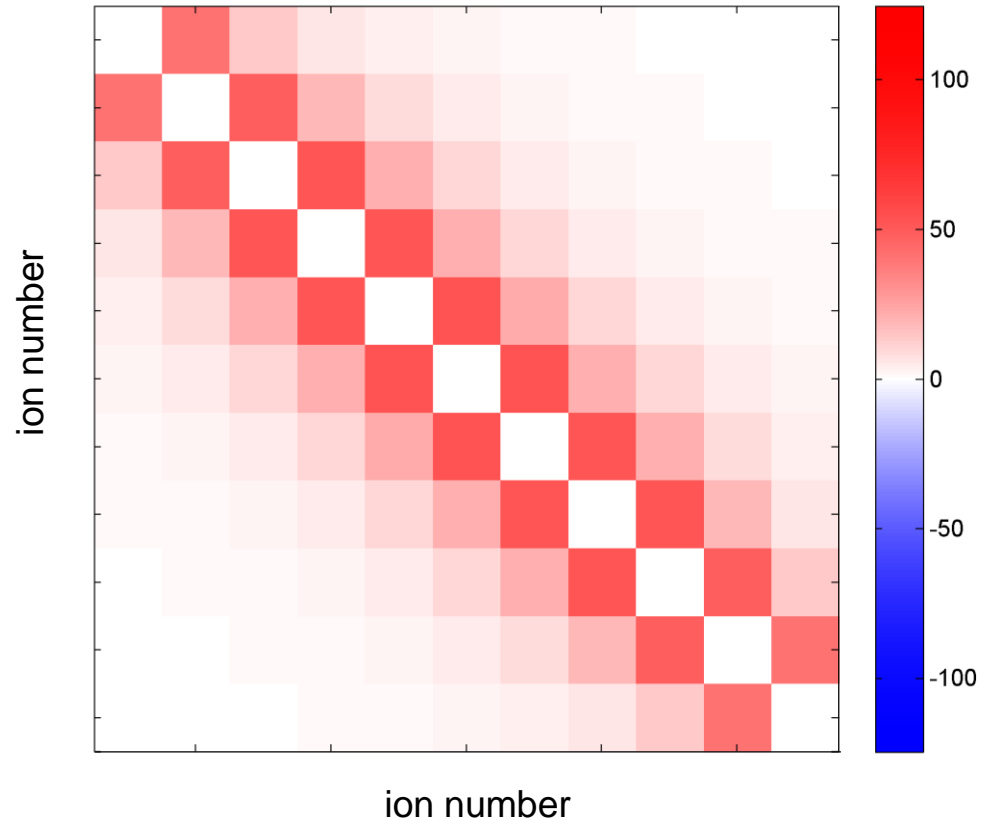
Example: 11 ions

$$J_{ij} = \Omega^2 \frac{(\hbar k)^2}{2m} \sum_m \frac{b_{i,m} b_{j,m}}{\Delta^2 - \nu_m^2}$$

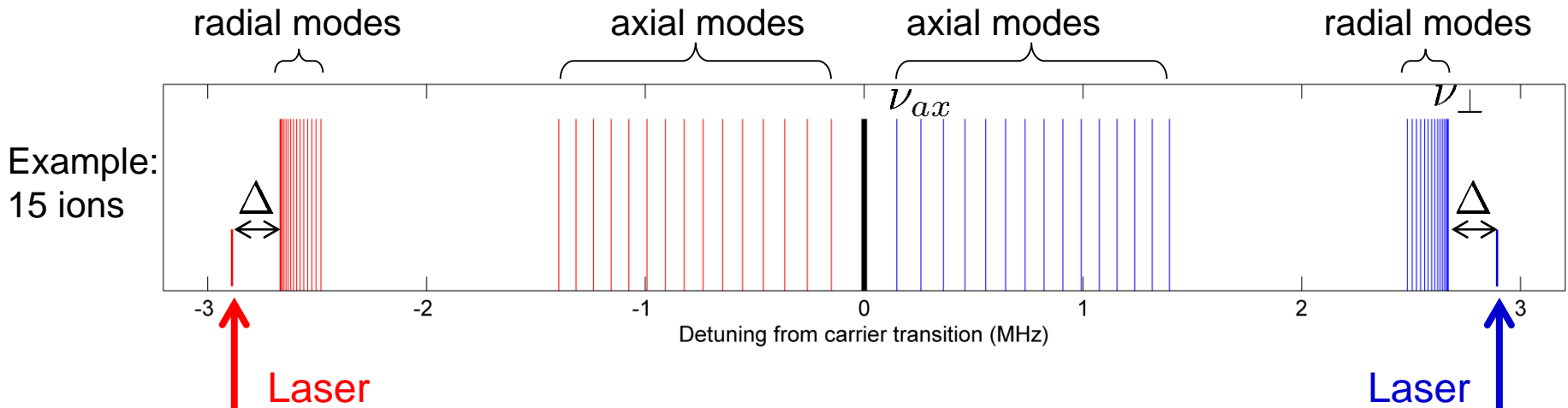
vibrational mode



Spin-spin coupling matrix J_{ij} (Hz)



Variable-range interactions by coupling to transverse modes



$$H = \sum_{i < j} J_{ij} \sigma_i^x \sigma_j^x \quad \text{with} \quad J_{ij} \approx \frac{J_0}{|i - j|^\alpha}$$

Interaction range: $0 < \alpha < 3$

couple only to
center-of-mass

couple to all modes
equally

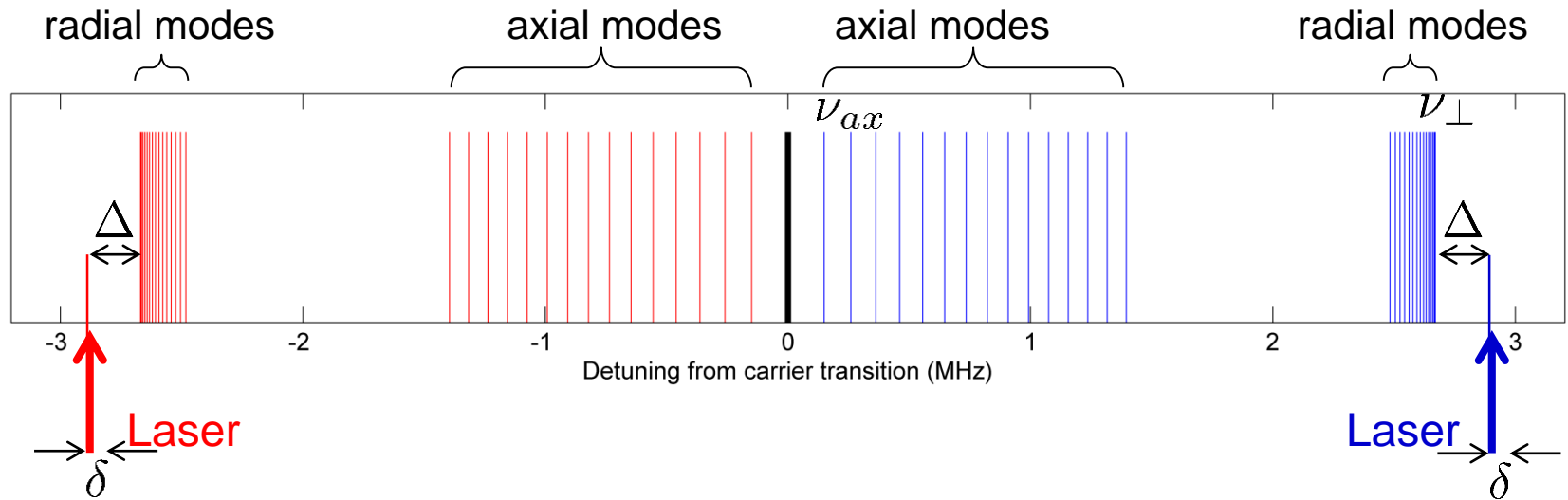
Knobs to turn:

- laser detuning Δ
- spread of radial modes

K. Kim et al, PRL **103**, 120502 (2009)

J. Britton et al, Nature **484**, 489 (2012)

Ising model with transverse field



$$H = \sum_{i < j} J_{ij} \sigma_i^x \sigma_j^x + B \sum_i \sigma_i^z \quad B = \delta/2$$

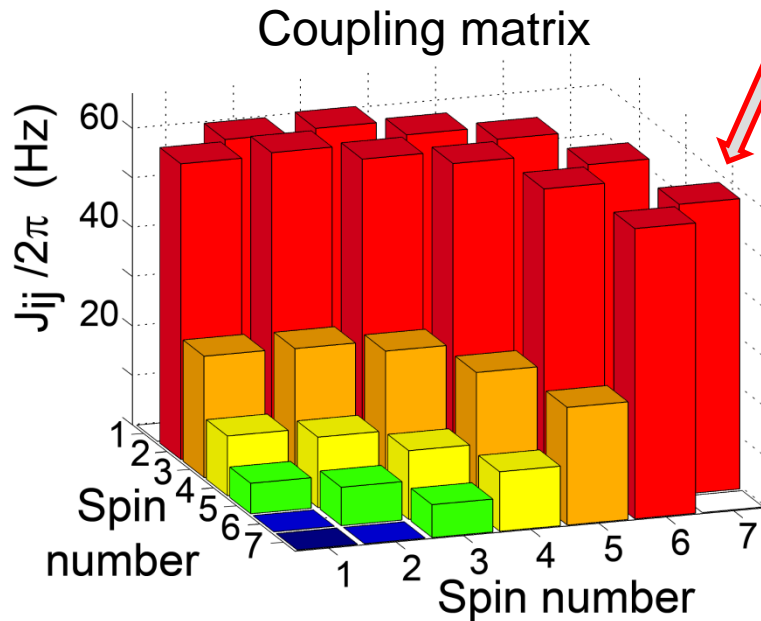
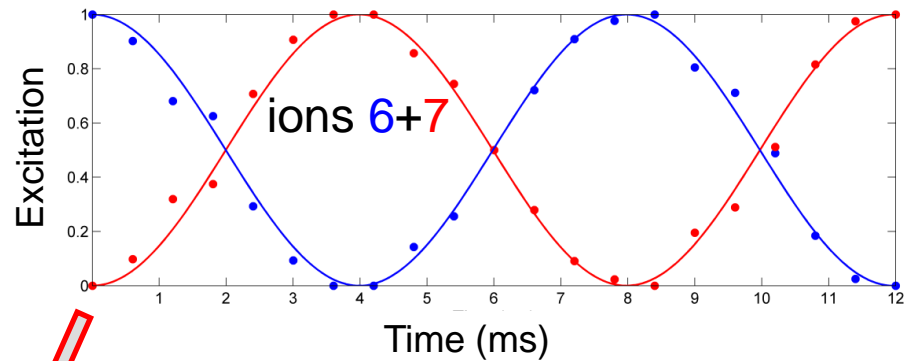
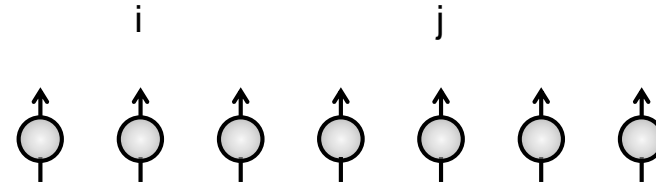
$$\approx \sum_{i < j} J_{ij} (\sigma_i^+ \sigma_j^- + h.c.) + B \sum_i \sigma_i^z \quad \text{for } B \gg J$$

„XY model“: hopping of spin excitations

Measurement of the coupling matrix

Protocol:

1. Initialize ions in state $|\uparrow\rangle_i |\downarrow\rangle_j$
2. Switch on Ising Hamiltonian
 $|\uparrow\rangle_i |\downarrow\rangle_j \longleftrightarrow |\downarrow\rangle_i |\uparrow\rangle_j$
3. Measure coherent hopping rate



Spread of correlations after local quenches

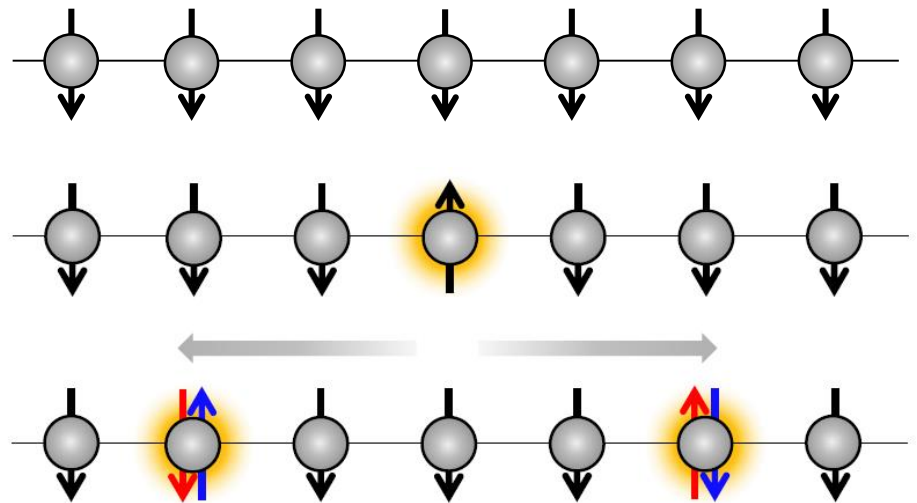
$$H_{XY} = \sum_{i < j} J_{ij} (\sigma_i^+ \sigma_j^- + h.c.) + B \sum_i \sigma_i^z$$

Ground state: all spins aligned with transverse field

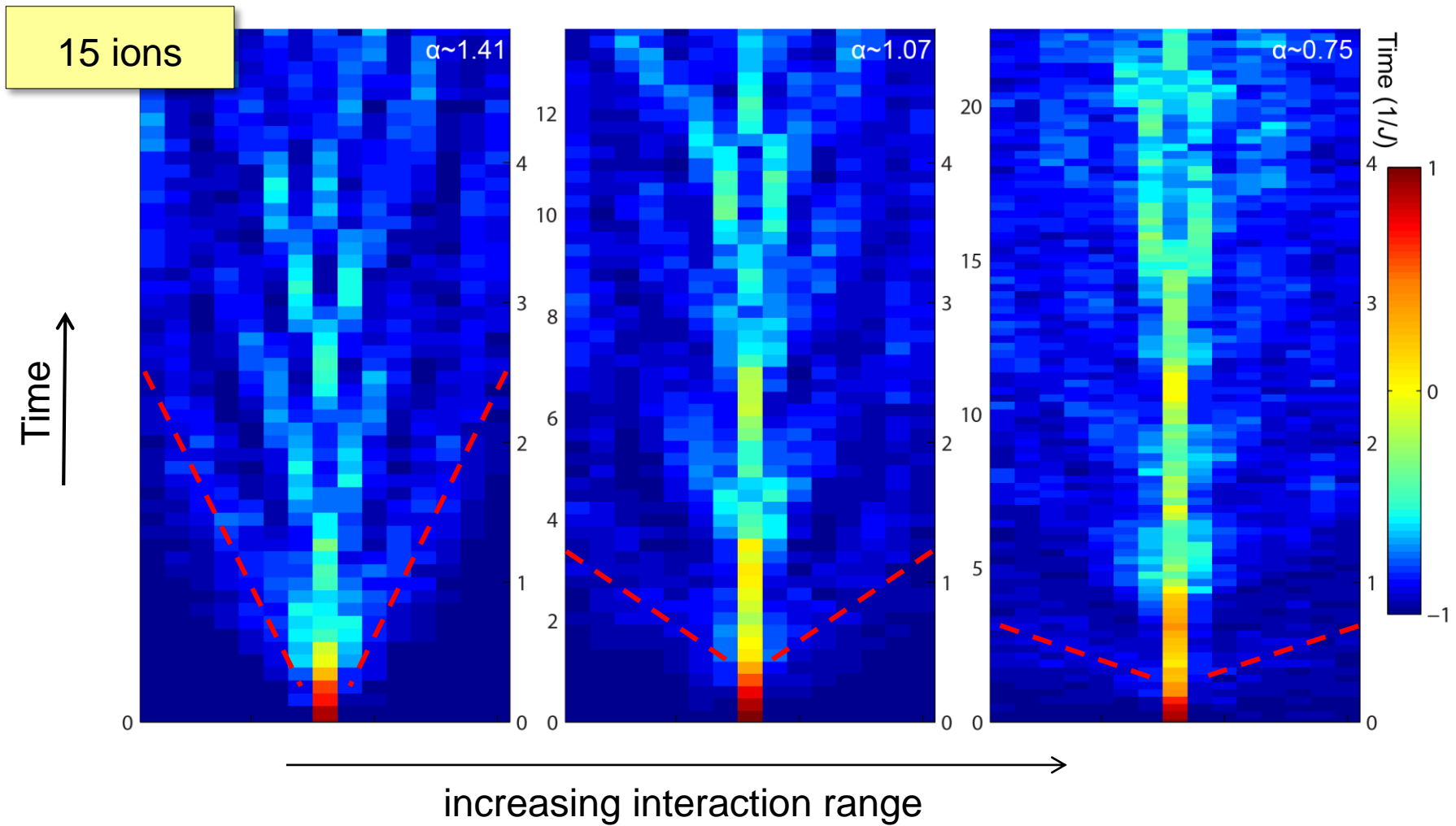
1. Local quench: flip one spin

2. Spread of entanglement

3. Measure magnetization or spin-spin correlations



Magnetization dynamics after a local quench

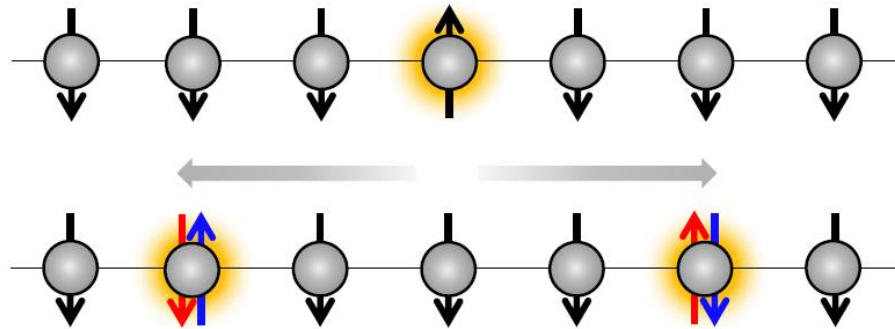


P. Jurcevic et al., Nature **511**, 202 (2014)

see also: P. Richerme et al., Nature **511**, 198 (2014)

$$J_{ij} \approx J_0 \frac{1}{|i - j|^\alpha}$$

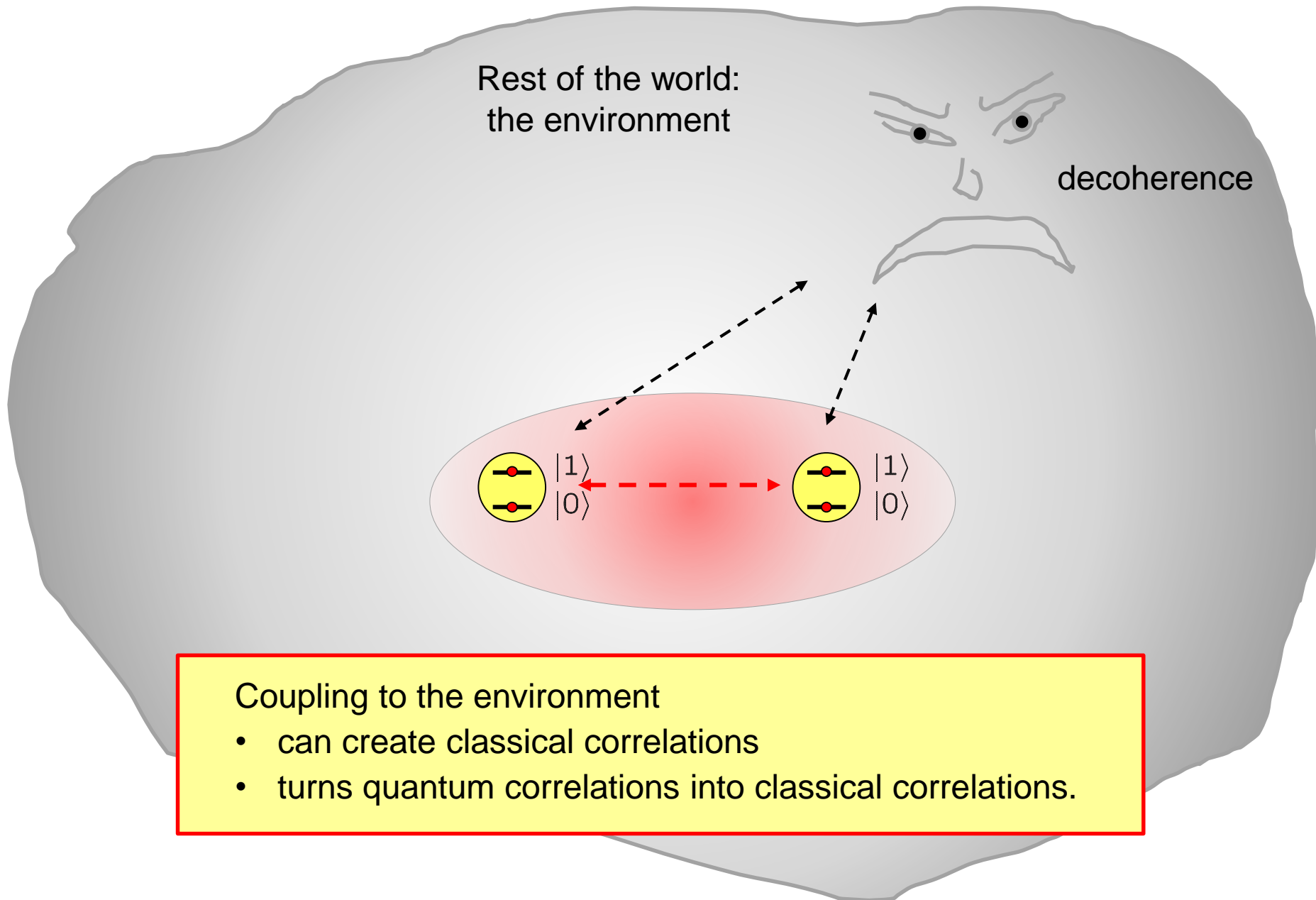
Entanglement generation in many-body dynamics



The quantum dynamics induced by a many-body Hamiltonian creates entanglement.

How can we demonstrate that this really happens in our experiment?

Classical vs quantum correlations



Classical vs quantum correlations

Example: Comparison of two different states

$$\Psi_- = \frac{1}{\sqrt{2}}(|\uparrow\downarrow\rangle - |\downarrow\uparrow\rangle)$$

$|\uparrow\downarrow\rangle$ or $|\downarrow\uparrow\rangle$
50% 50%

Both state have the same expectation values when measured in z-basis:

$$\langle\sigma_z^{(i)}\rangle = 0$$
$$\langle\sigma_z^{(1)}\sigma_z^{(2)}\rangle = -1$$

Only measurements along x or y reveal the difference:

$$\langle\sigma_x^{(1)}\sigma_x^{(2)}\rangle = -1$$
$$\langle\sigma_x^{(1)}\sigma_x^{(2)}\rangle = 0$$
$$\langle\sigma_y^{(1)}\sigma_y^{(2)}\rangle = -1$$
$$\langle\sigma_y^{(1)}\sigma_y^{(2)}\rangle = 0$$

Detecting entanglement

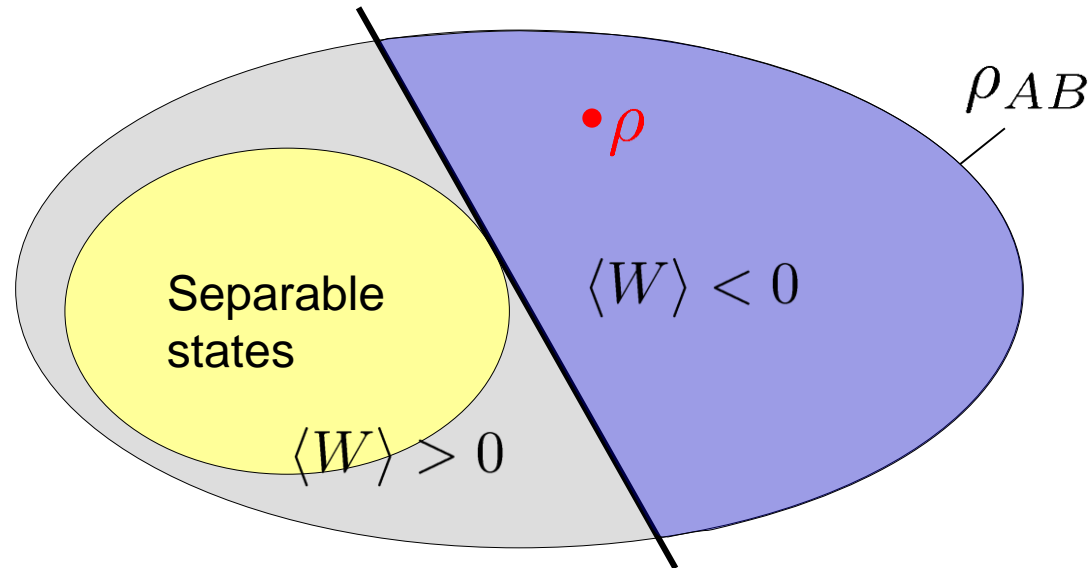
Deciding whether a state is entangled or not is a hard task.

Entanglement detection techniques:

- **Positive partial trace (PPT) criterion**: check whether a **density matrix** after partial transposition has negative eigenvalues.
- **Entanglement witnesses**: Particular **observables** that have negative expectation value for some entangled states, but are positive for separable states.
- **Entanglement measures (for example: concurrence)**:
Nonlinear functions of the **density matrix** that are zero for separable mixed states and positive for entangled states.
Entanglement measures quantify entanglement but can be hard to calculate even if the density matrix is known; for two qubits, closed expressions exist.

Detecting entanglement by witness operators

Quantum states of a composite quantum system



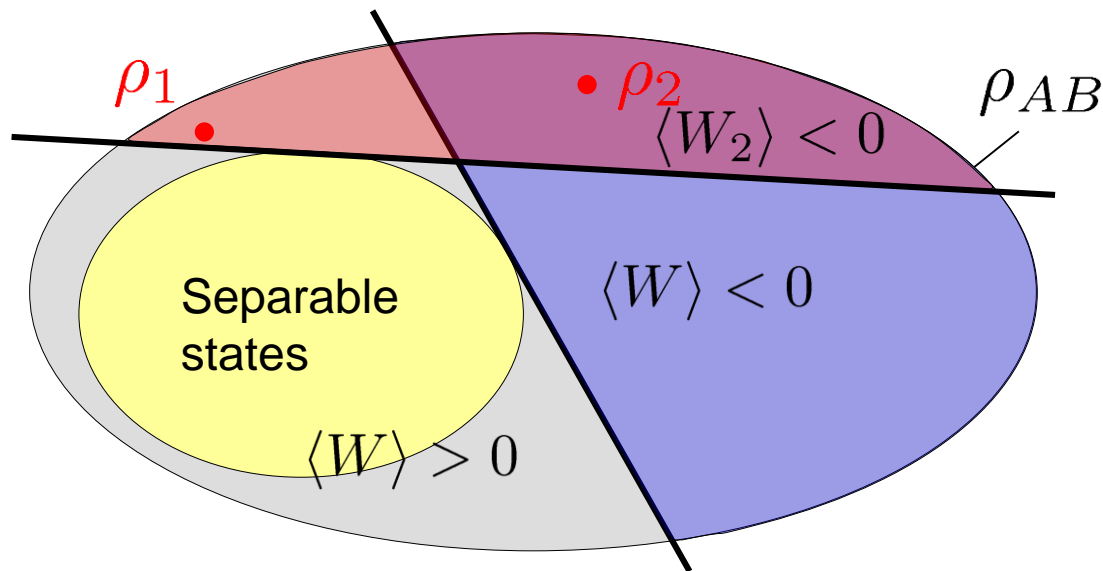
Witness: An observable W whose expectation value is positive for all separable states

$$\langle W \rangle = \text{Tr}(\rho W) \geq 0$$

If we measure $\langle W \rangle < 0$ in an experiment, we can conclude that the state is entangled.

Detecting entanglement by witness operators

Quantum states of a composite quantum system



- Not every entangled state is detected by a witness

→ ρ_1

$$\text{Tr}(\rho_1 W) \geq 0$$

- An entangled state can be detected by more than one witness

→ ρ_2

$$\text{Tr}(\rho_2 W) < 0 \quad \text{Tr}(\rho_2 W_2) < 0$$

Tomographic reconstruction of the density matrix

Representation of ρ as a sum of orthogonal observables A_i :

$$\rho = \sum_i \lambda_i A_i \quad \text{with} \quad \text{Tr}(A_i A_j) = \delta_{ij}$$

ρ is completely determined by the expectation values $\langle A_i \rangle$:

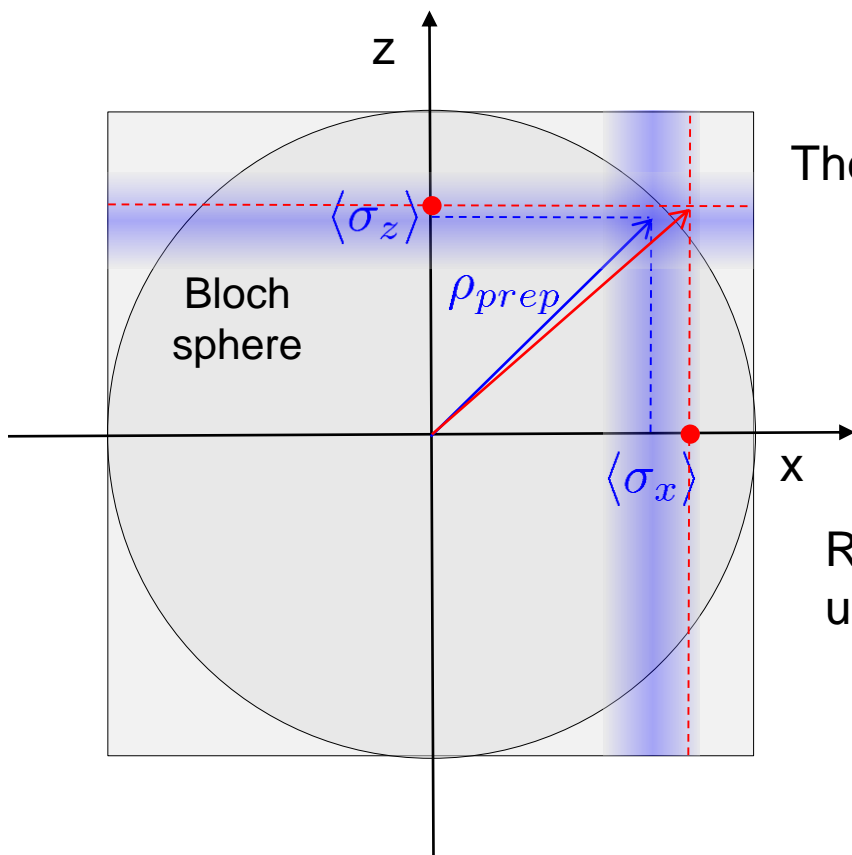
$$\langle A_j \rangle = \text{Tr}(\rho A_j) = \sum_i \lambda_i \text{Tr}(A_i A_j) = \lambda_j$$

For a two-ion system : $A_i \in \{\sigma_i^{(1)} \otimes \sigma_j^{(2)}, \sigma_i \in \{I, \sigma_x, \sigma_y, \sigma_z\}\}$

—————> Joint measurements of all spin components $\sigma_i^{(1)} \otimes \sigma_j^{(2)}$

$$\rho_R = \sum_{i=1}^{16} \langle A_i \rangle A_i$$

Example: Tomography of a qubit



The experimental procedure prepares the state ρ_{prep}

$$\rho_{prep} = \frac{1}{2}(I + \langle \sigma_x \rangle \sigma_x + \langle \sigma_y \rangle \sigma_y + \langle \sigma_z \rangle \sigma_z)$$

Reconstruction by estimation of $\langle \sigma_x \rangle, \langle \sigma_y \rangle, \langle \sigma_z \rangle$ using a finite number of copies of the state:

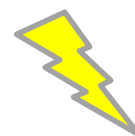
$$s_z = \frac{N_{\uparrow} - N_{\downarrow}}{N_{\uparrow} + N_{\downarrow}}, \quad s_x = \dots, \quad s_y = \dots$$

$$\rho_{tomo} = \frac{1}{2}(I + s_x \sigma_x + s_y \sigma_y + s_z \sigma_z) \neq \rho_{prep}$$

ρ_{tomo} might not be within the Bloch sphere !

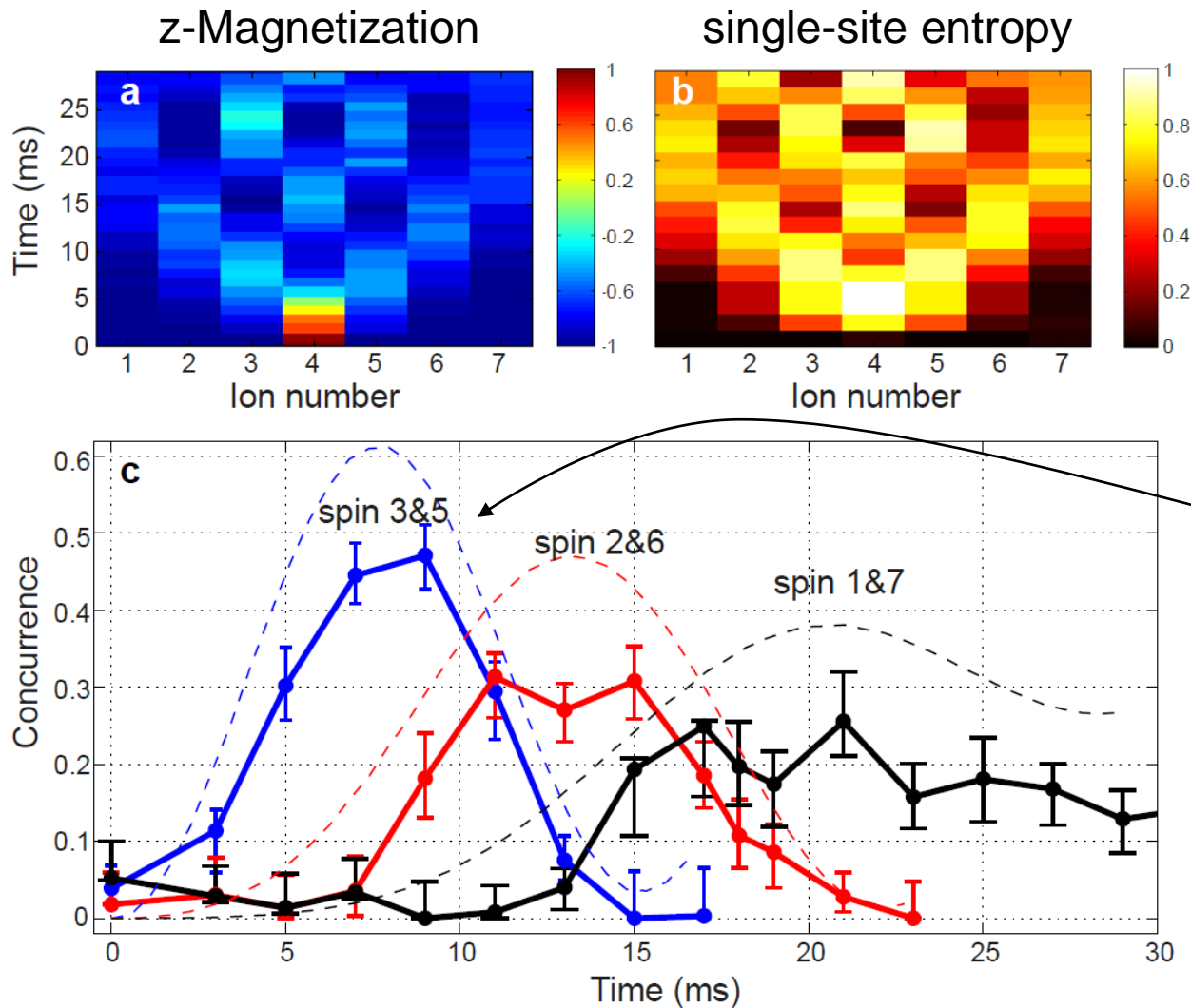


DISASTER !!!

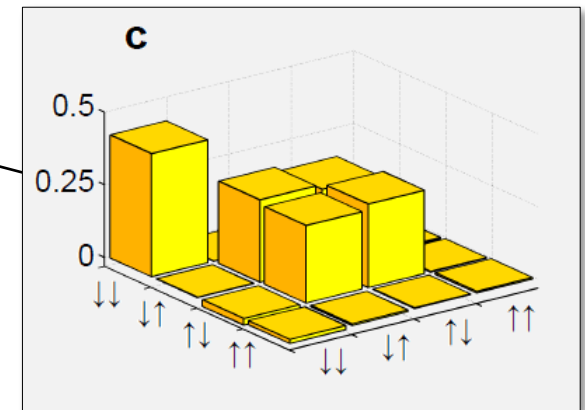


Nonlinear combination of measurement results!

Spread of entanglement after a local quench



7 ions
 $a \approx 1.75$



density matrix reconstruction
 of spins 3 + 5
 9 ms after the quench

$$\mathcal{F} = \text{Tr}(\rho|\psi\rangle\langle\psi|) = 0.975$$

Characterization of large complex entangled states

20 ions

Time ↑

Questions to be answered:

- Highly entangled state or noisy mess?
- How to characterize entangled states with >8 ions?
- How coherent is the engineered spin-spin interaction?

Ion number

2

4

6

8

10

12

14

16

18

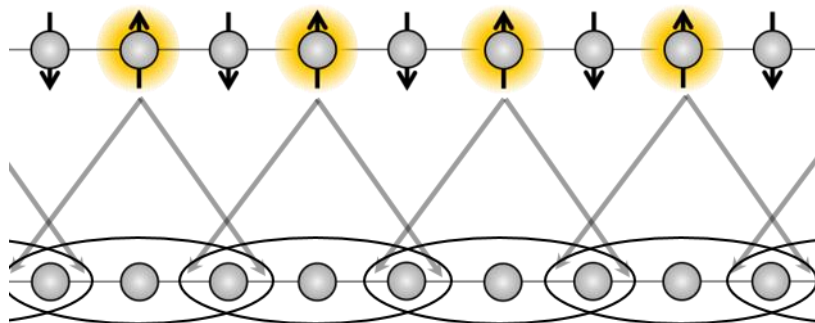
20

Characterization of large complex entangled states

20 ions

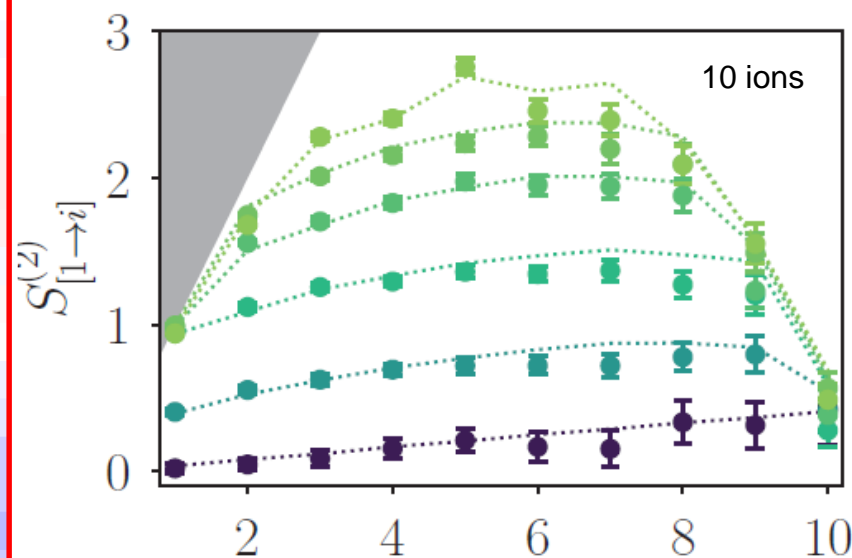
Time ↑

Matrix-product state tomography



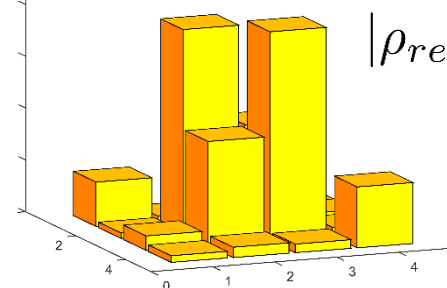
B. Lanyon *et al.*, Nat. Phys. **13**, 1158 (2017)

Entropy measurements by random unitaries



T. Brydges *et al.*, Science **364**, 260 (2019)

Quantum state tomography of subsystems



N. Friis *et al.*, PRX **8**, 021012 (2018)

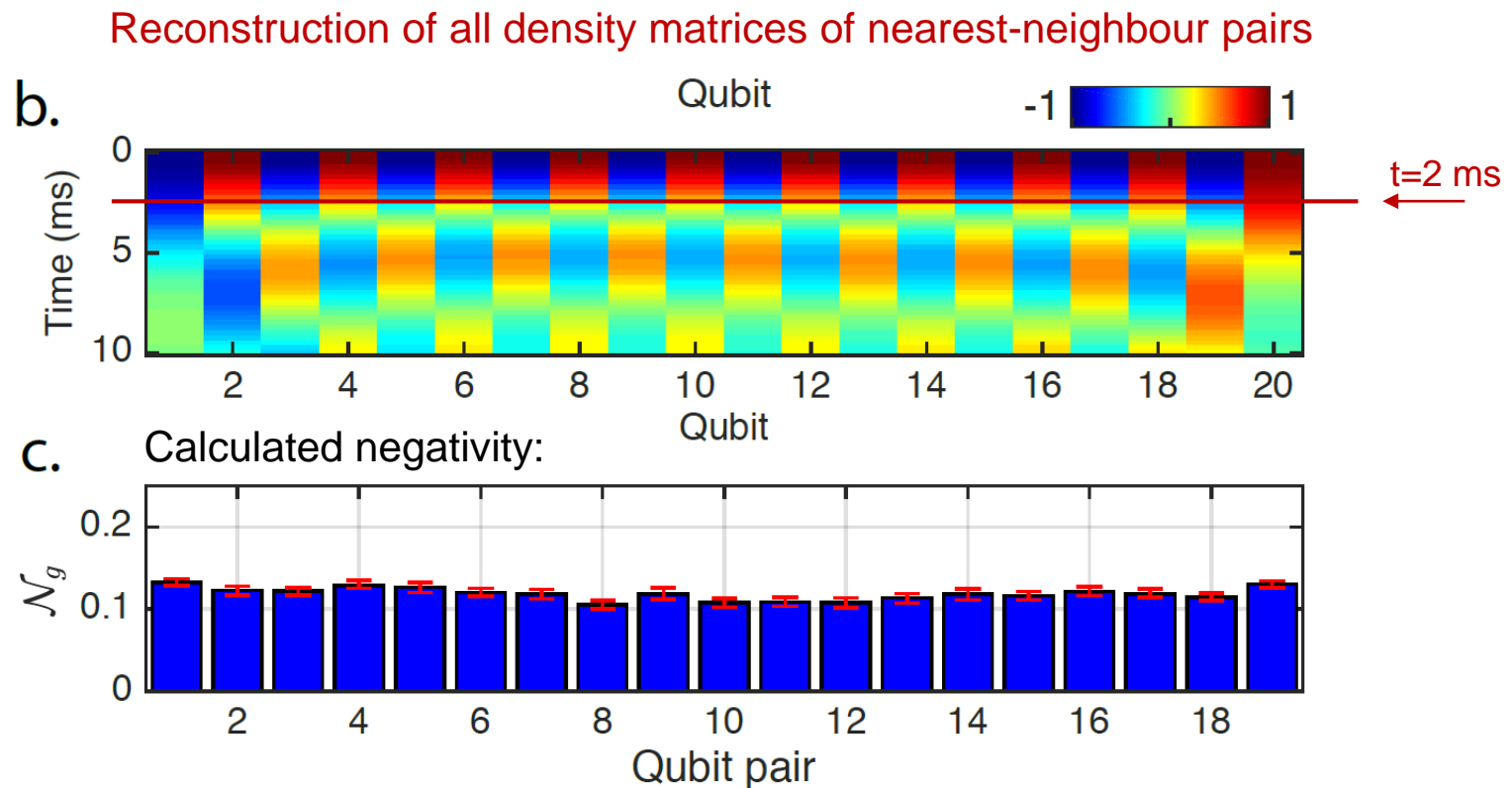
Ion number

2 4 6 8 10 12 14 16 18 20

Entanglement detection in multi-ion experiments

Local characterization of the beginning of entanglement spreading

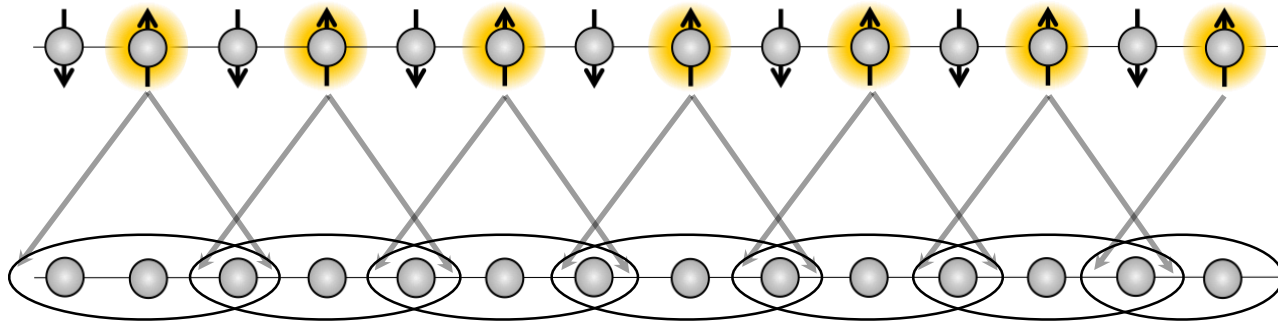
Option 1: Quantum state tomography to reconstruct the density matrix of subsystems



→ After 2 ms of time evolution, all ions are entangled with their neighbours

Entanglement detection in multi-ion experiments

Local characterization of the beginning of entanglement spreading

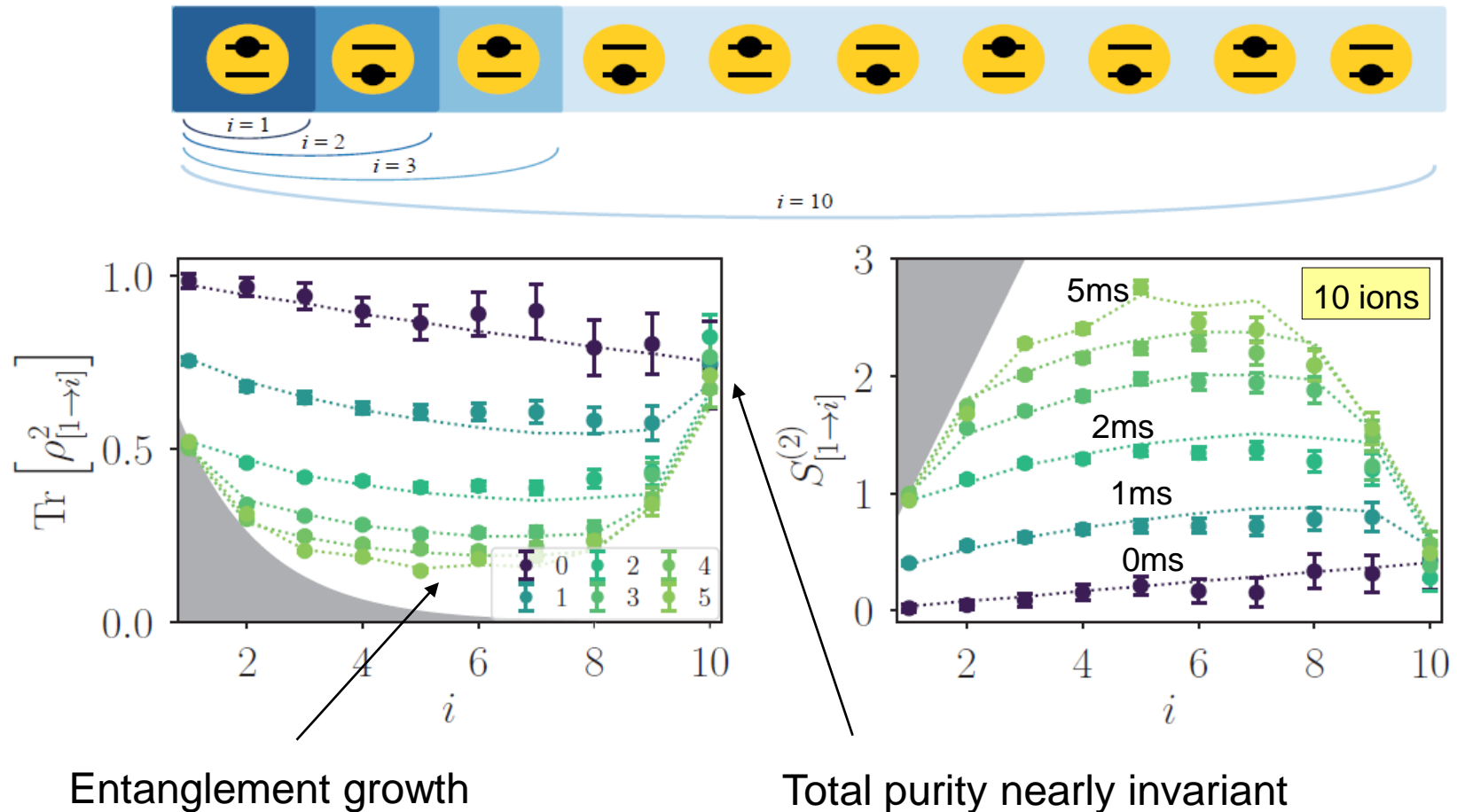


Option 2: Measure all correlation functions between groups of neighbouring ions (pairs, triplets,...) and try to build up a global representation of the quantum state using a suitable parametrization of the state

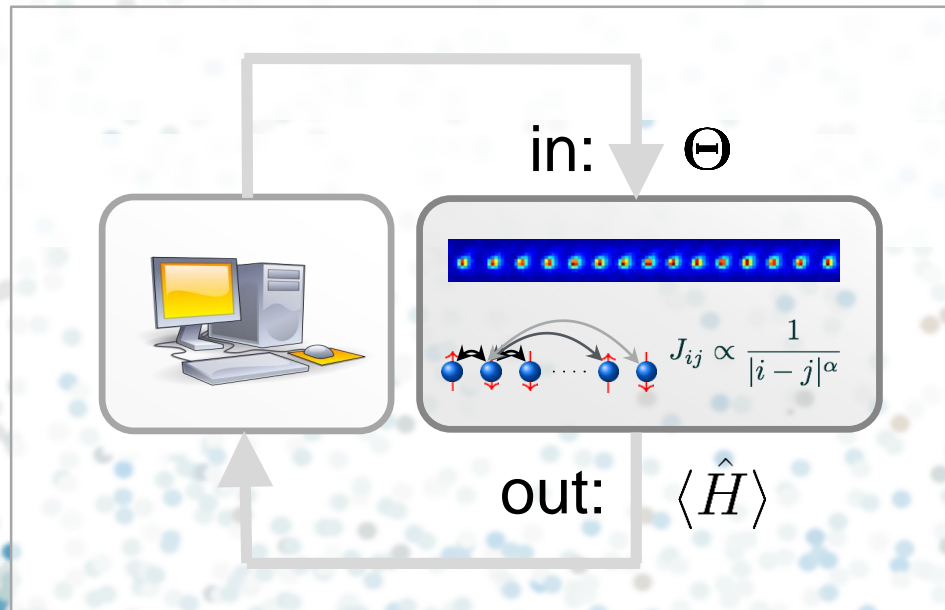
→ Matrix product state tomography

Entanglement detection in multi-ion experiments

Option 3: Compare the purity of density matrices describing subsystems to the purity of the overall density matrix

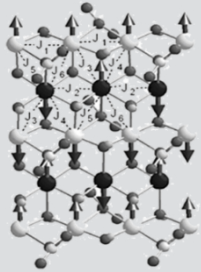


Entanglement as a computational resource: Variational quantum simulation



Variational quantum simulation

Target



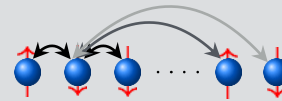
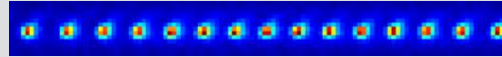
spin Hamiltonian

$$\hat{H}_T = \sum_{n=1}^M \hat{h}_n$$

$$\hat{h}_n = a_n \hat{\sigma}_i^x \hat{\sigma}_j^y \hat{\sigma}_k^z \dots$$

→ sums of Pauli products:

Quantum Resource

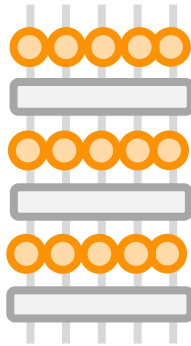


$$J_{ij} \propto \frac{1}{|i-j|^\alpha}$$

$$U_1(\Theta) = \exp \left(-i\Theta \sum_{i<j} J_{ij} (\sigma_i^+ \sigma_j^- + \text{h.c.}) \right)$$

$$U_{2,i}(\Theta) = \exp (-i\Theta \sigma_i^z)$$

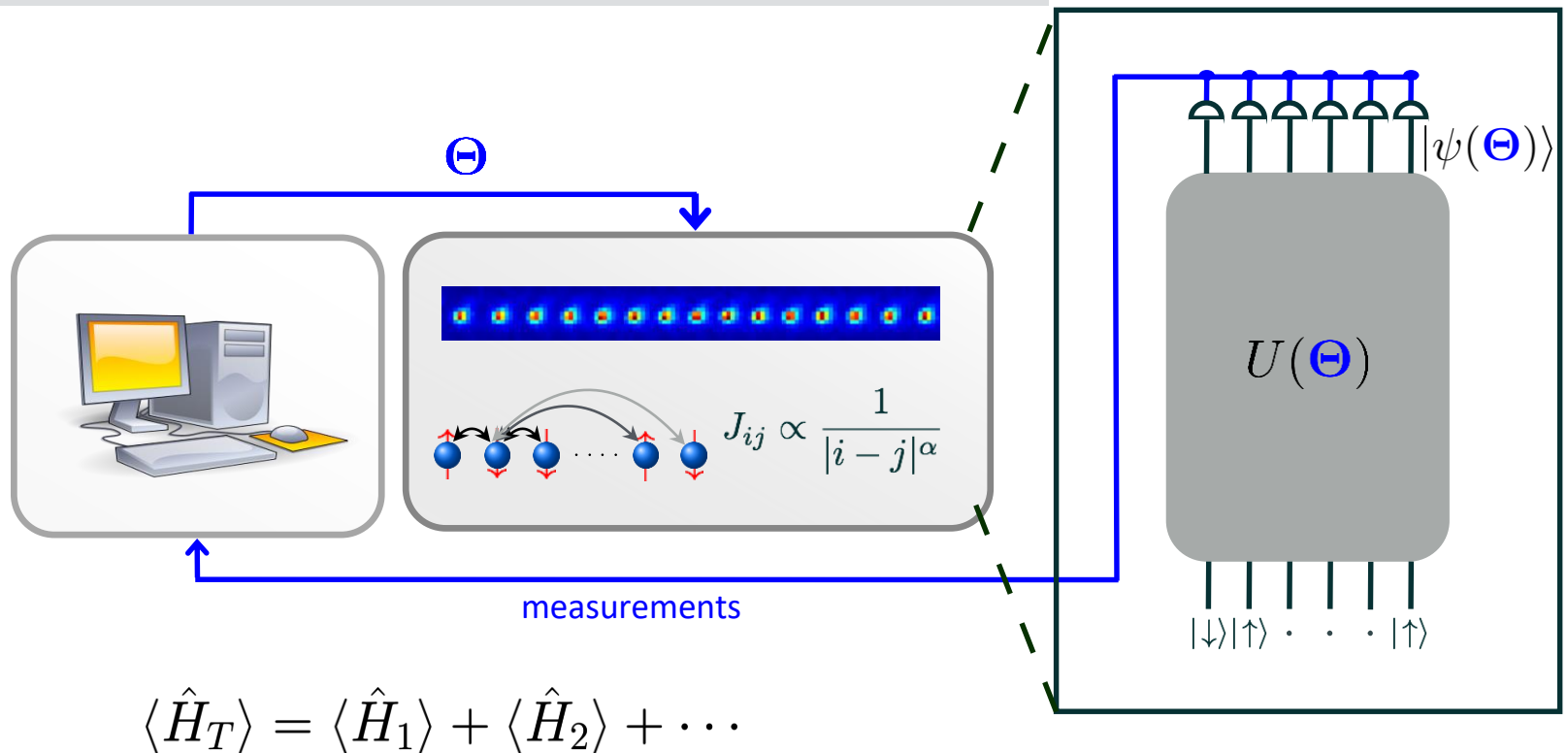
$$|\psi(\Theta)\rangle = \hat{U}_N(\Theta_N) \dots \hat{U}_2(\Theta_2) \hat{U}_1(\Theta_1) |\psi_0\rangle$$



Variational quantum simulation

The goal of Variational Quantum Simulation

Prepare ground state of \hat{H}_T by minimising $\langle \psi(\Theta) | \hat{H}_T | \psi(\Theta) \rangle$

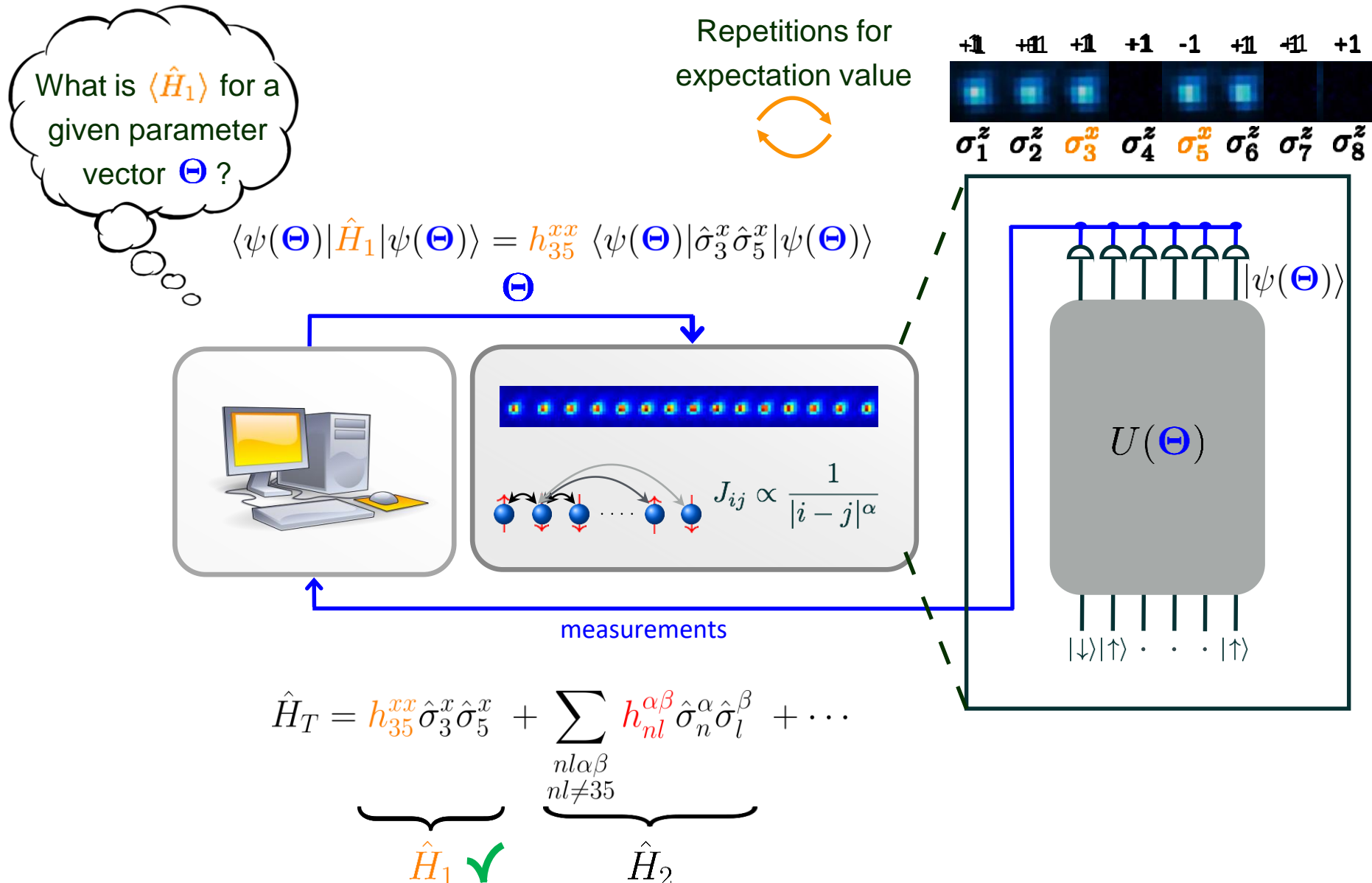


Peruzzo et al., Nature Comm. 5, 4213 (2014)

Farhi et al., arXiv:1411.4028 (2014)

McClean et al., NJP 18, 023023 (2016)

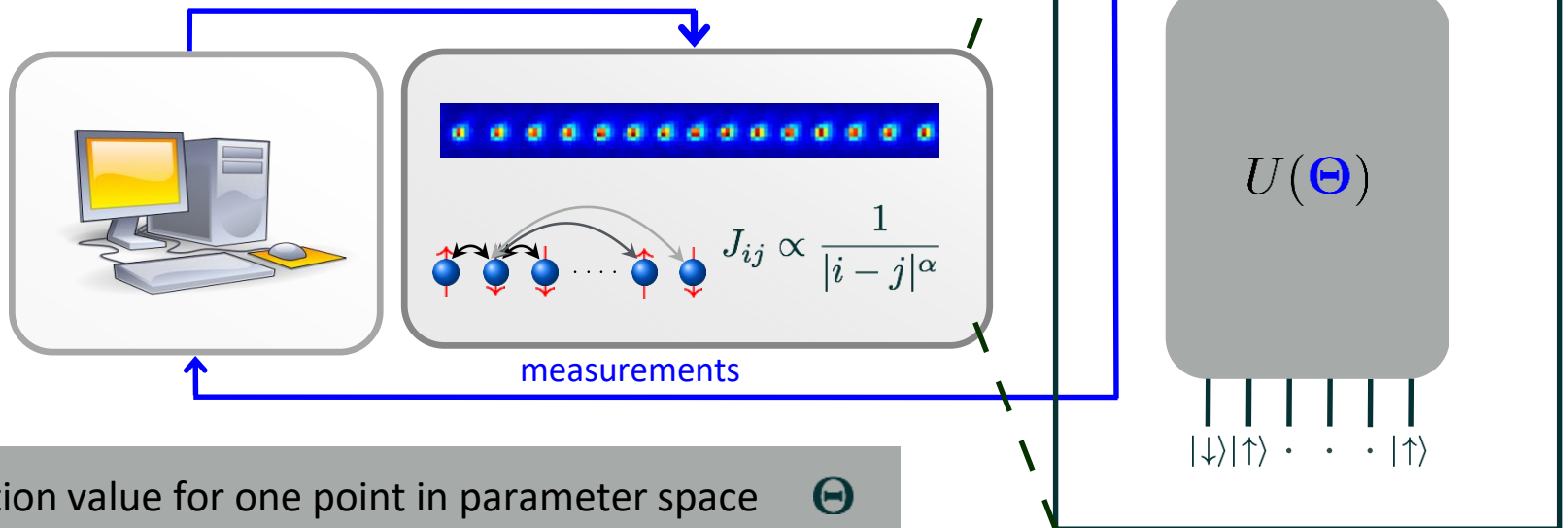
Variational quantum simulation



Variational quantum simulation

What is $\langle \hat{H}_1 \rangle$ for a given parameter vector Θ ?

$$\langle \psi(\Theta) | \hat{H}_1 | \psi(\Theta) \rangle = h_{35}^{xx} \langle \psi(\Theta) | \hat{\sigma}_3^x \hat{\sigma}_5^x | \psi(\Theta) \rangle$$



Expectation value for one point in parameter space Θ

$$\langle \psi(\Theta) | \hat{H}_T | \psi(\Theta) \rangle = \underbrace{\langle \hat{H}_1 \rangle}_{\hat{H}_1 \checkmark} + \underbrace{\langle \hat{H}_2 \rangle}_{\hat{H}_2} + \dots$$

Quantum resources for variational search: ground state energy of Schwinger lattice model

Entangling operations

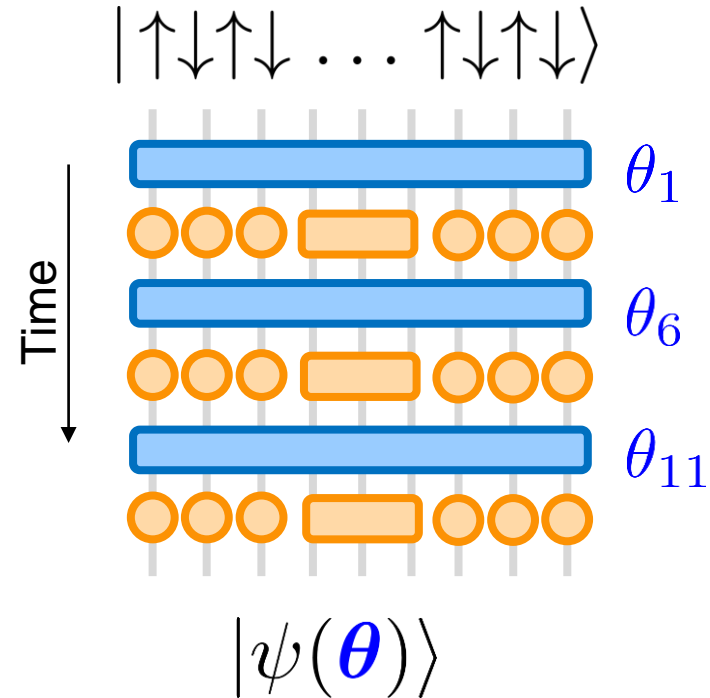
$$U(\theta) = \exp(i\theta \sum_{i < j} J_{ij} (\sigma_i^+ \sigma_j^- + \sigma_i^- \sigma_j^+))$$

Single-qubit rotations

$$U(\theta) = \exp(i\theta \sigma_i^z)$$

Collective qubit rotations

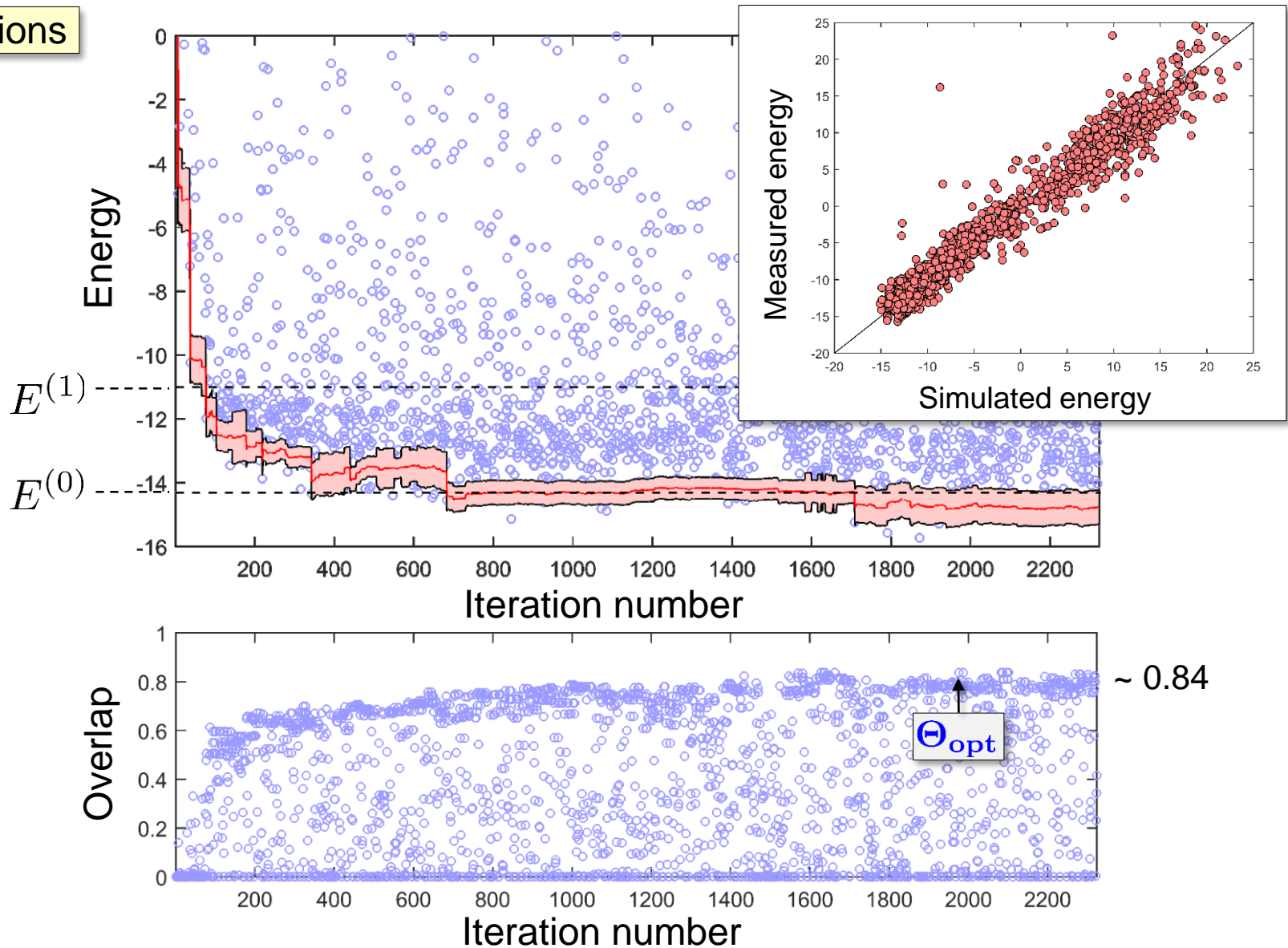
$$U(\theta) = \exp(i\theta \sum_i \sigma_i^x)$$



20 ions, 6 layers of operations, 15 variational parameters

Experimental results: energy minimization

20 ions

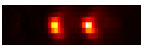


Scaling up trapped-ion quantum simulations


Options for experimenting with larger ion crystals:

Longer linear ion strings

2



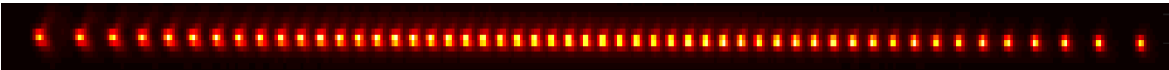
10



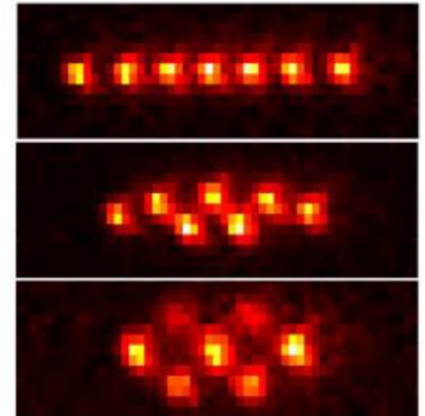
20



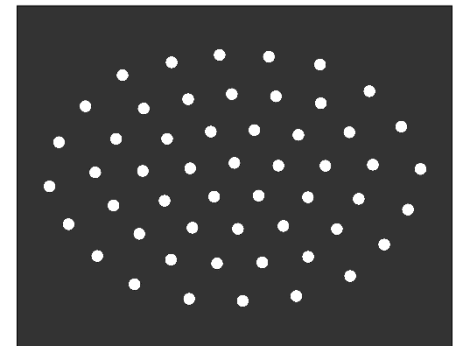
53



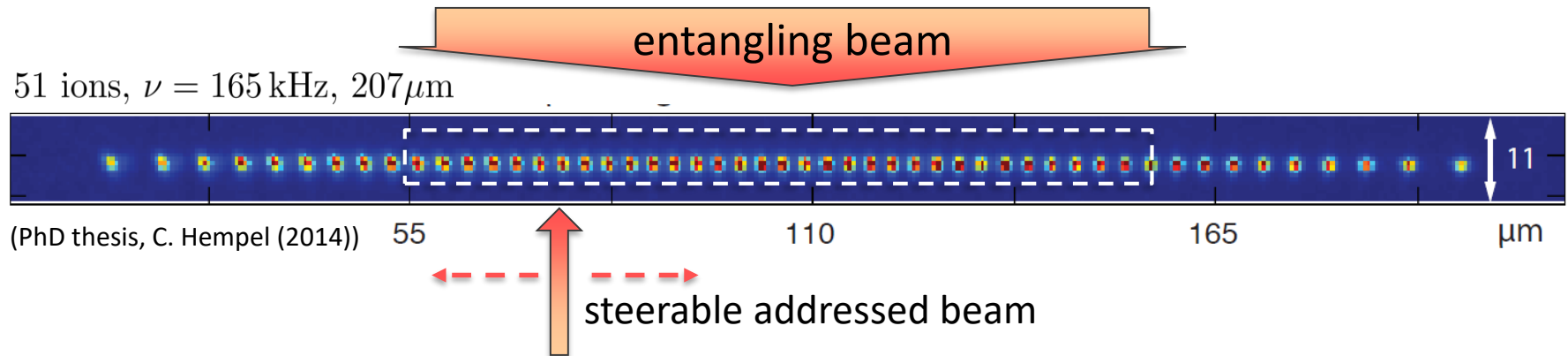
Two-dimensional crystals



53



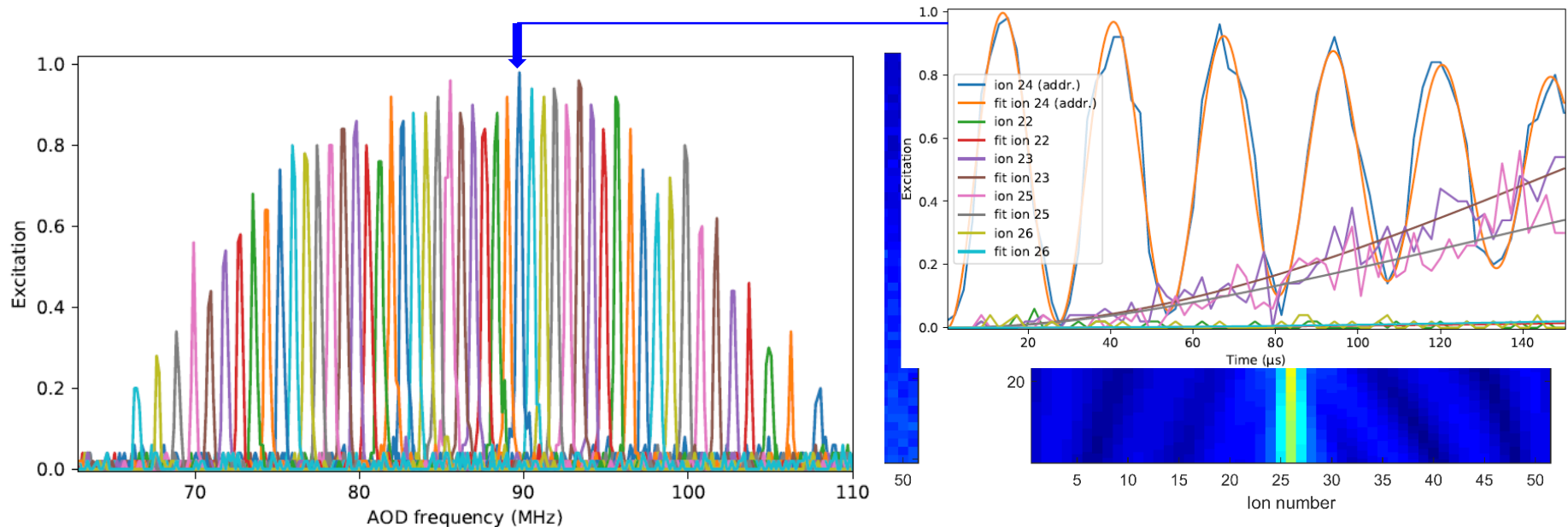
Ion strings with larger ion numbers:



Until very recently:

Only 20 ions fully controlled ions

Improved addressing setup ➡ 50 addressable ions



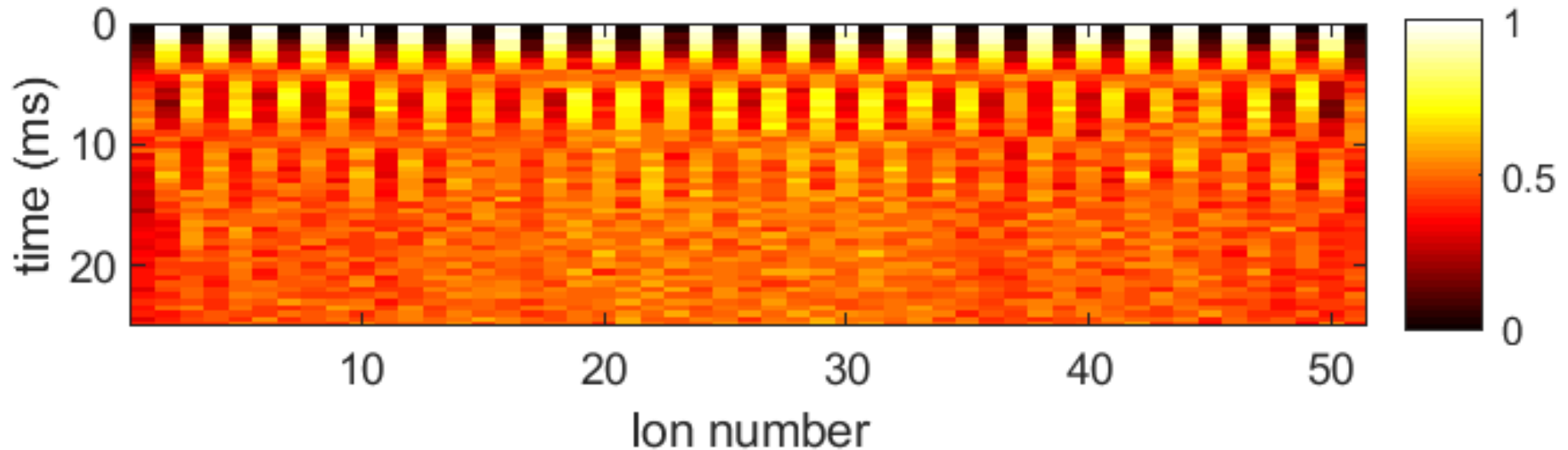
Entanglement in 50-ion strings

AOD

Néel state preparation with 60 % fidelity

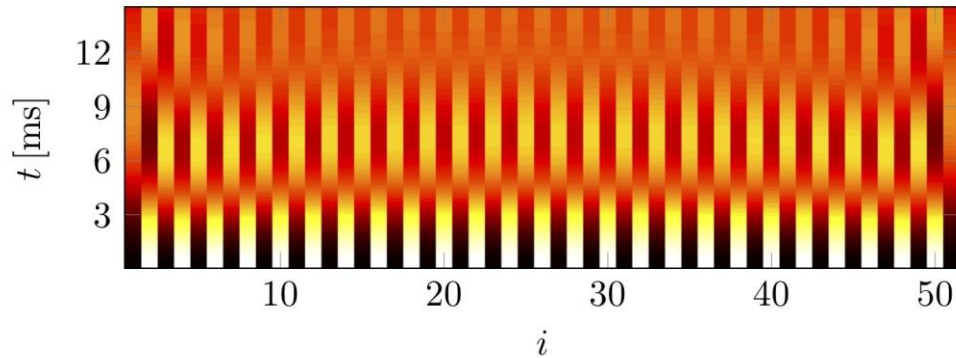


Néel-state dynamics under long-range XY model: z-magnetization

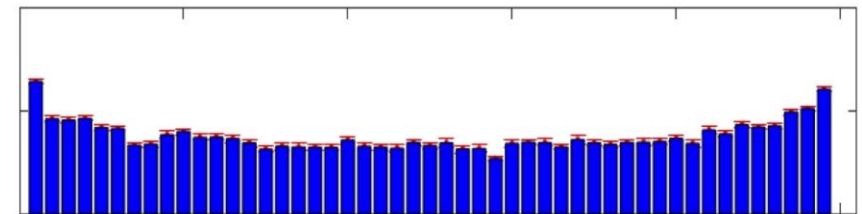
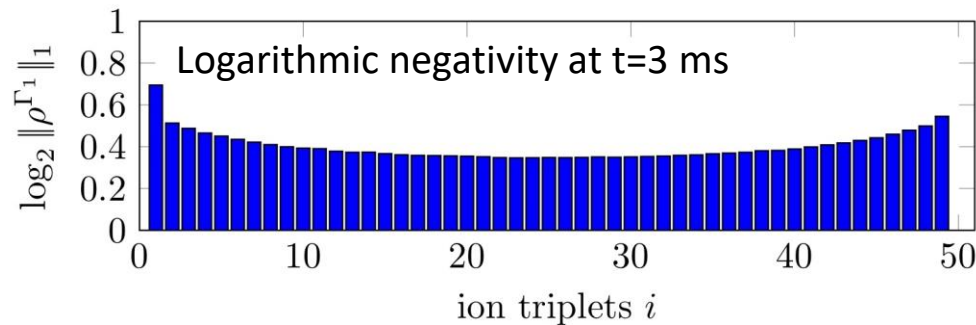
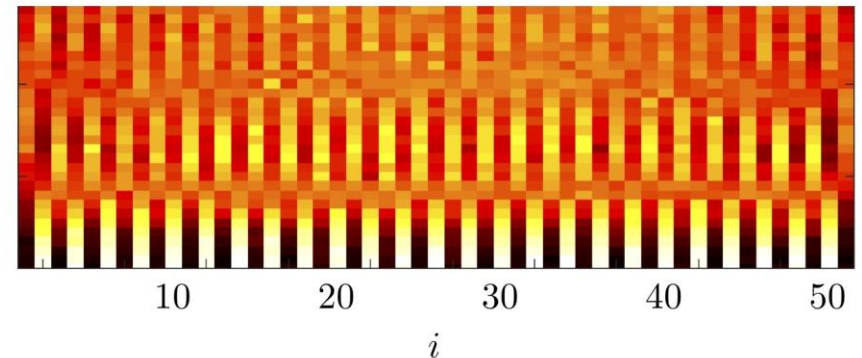


Entanglement in 50-ion strings

Theory (coherent dynamics)



Experiment



in collaboration with P. Zoller and co-workers

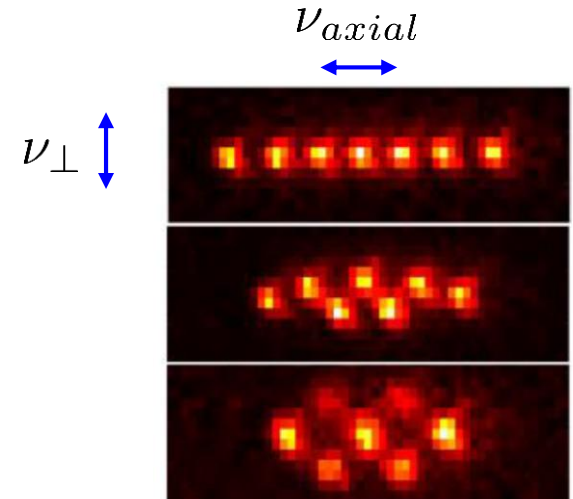
Scaling up trapped-ion quantum simulations

1d ion crystals:

- Very anisotropic trapping potentials needed for keeping the ion string linear:

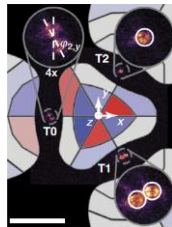
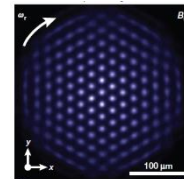
$$\nu_{\perp} / \nu_{axial} > N \log N$$

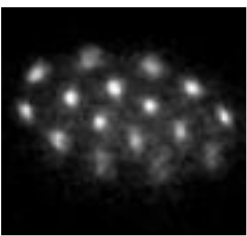
- low axial confinement
- tricky to control axial motion
- length of string complicates addressing



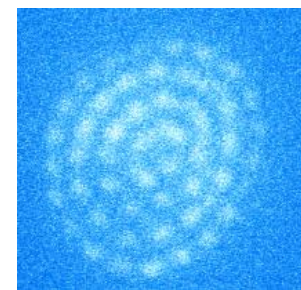
2d ion crystals:

- Penning traps → addressing of rotating crystals
- rf microtrap arrays → electric field noise due to proximity to trap surfaces
- rf linear trap → micromotion





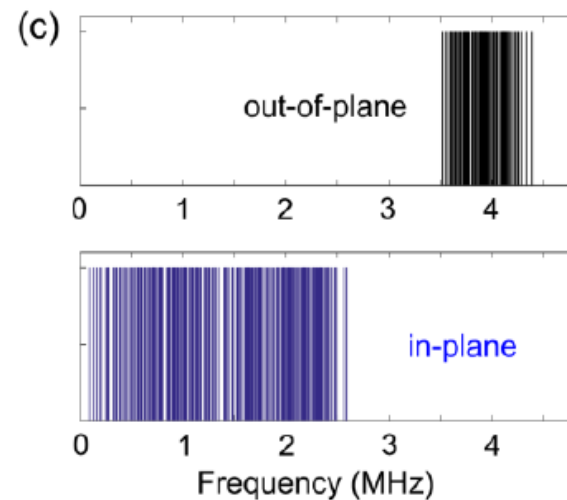
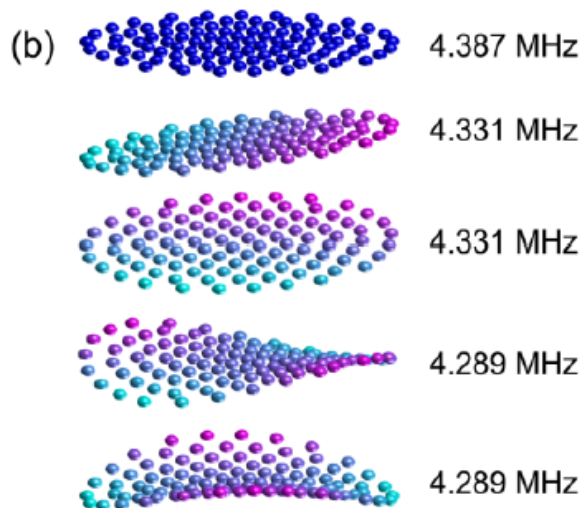
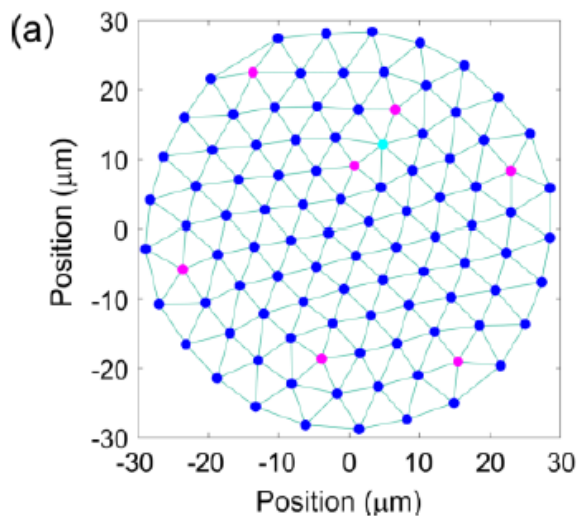
Planar ion crystals



(Campbell group, UCLA)

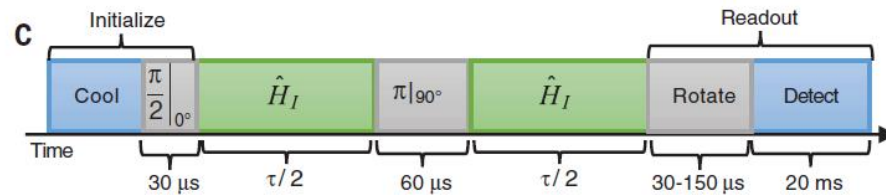
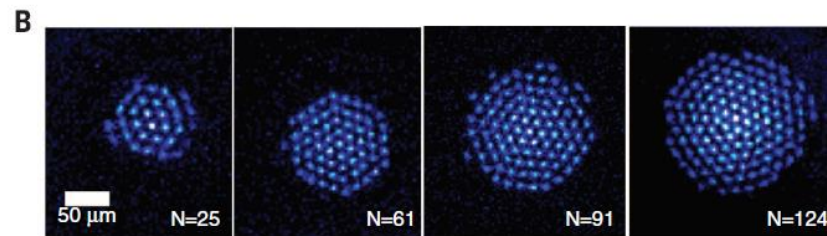
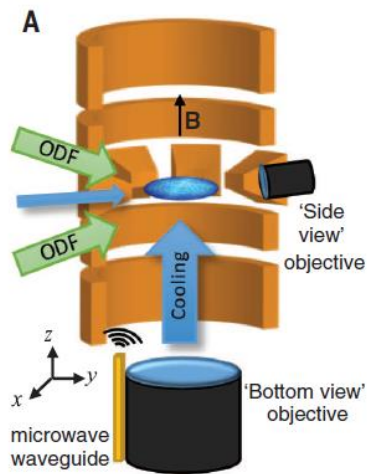
M. Block et al.
J. Phys. B **33**, L375 (2000)

Ions form triangular lattices with defects



Effective long-range spin-spin interactions by lasers coupling to the out-of-plane modes of vibration

Penning trap: spin dynamics in planar crystals



Experiment at NIST, Boulder (USA):

Quantum spin dynamics with >100 ions:

- Optical dipole force inducing spin squeezing
- Measurement of collective spin operators (rotating crystals)

J. G. Bohnet et al, Science 253, 1297 (2016)

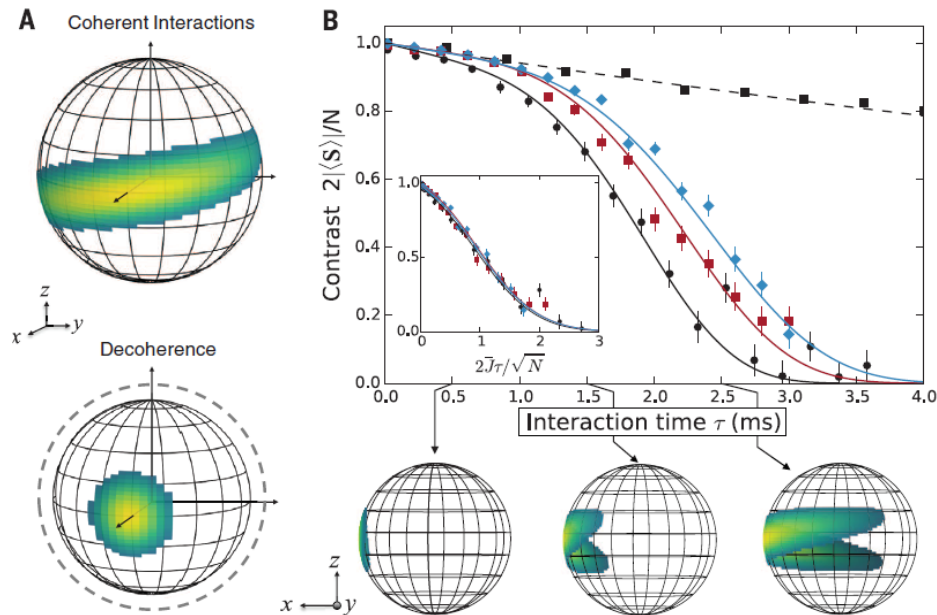
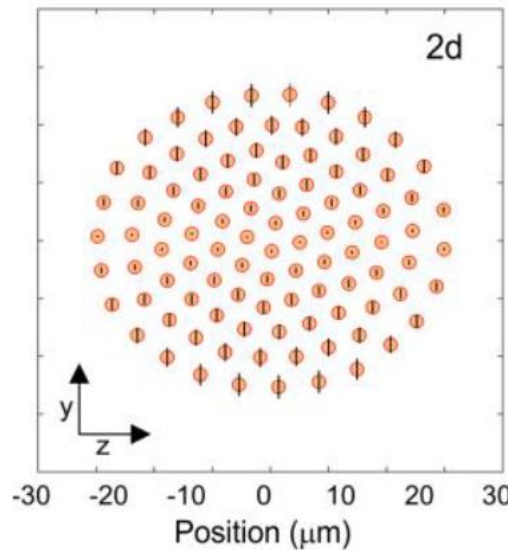
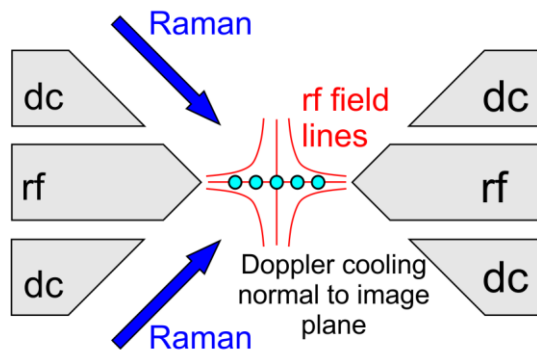
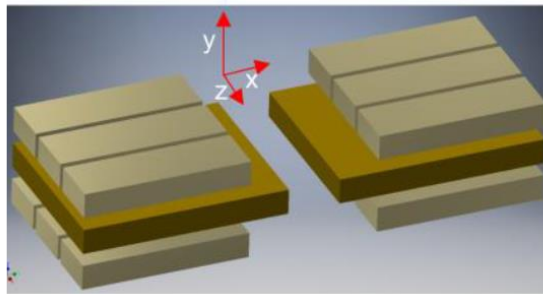
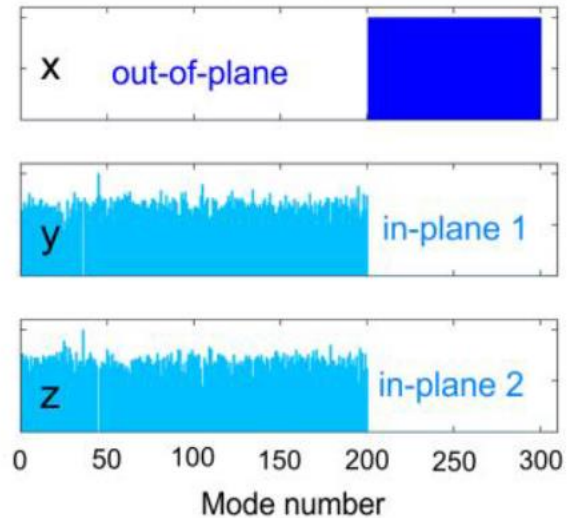


fig. 2. Depolarization of the collective spin from spin-spin interactions and decoherence. (A) The

Planar ion crystals in rf-traps: Micromotion



Normalized kinetic mode energy along principal axes



- no micromotion in direction of out-of-plane normal modes
- for certain geometries, laser cooling of in-plane modes not affected by MM

Spin-spin simulations with planar crystals in rf-traps

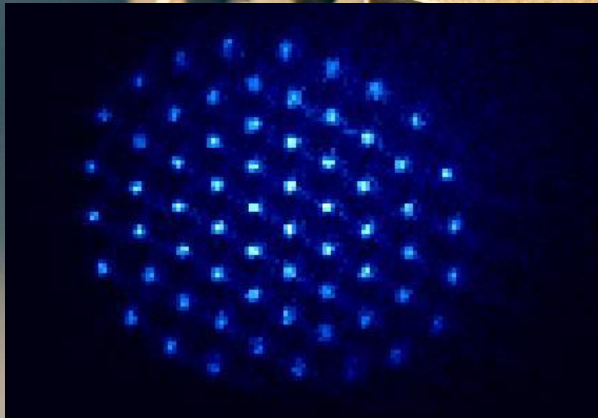


Challenges:

- melting of crystals by background gas collisions + recrystallization
- Laser cooling of in-plane modes
- Motional heating

New experiment:

- Monolithic ion trap
- Planar crystals trapped
- EIT ground-state cooling



Experiment along similar lines:

- Richerme group (Indiana Univ.)
- Kim group (Tsinghua Univ.)

Summary and outlook

Trapped-ion quantum simulations

- Quantum simulation approaches: digital vs analog
- Realization of long range spin models in trapped ions
- Entanglement creation and characterization in multi-ion strings
- Scaling up quantum simulations to larger ion numbers
- Variational quantum simulation

Outlook:

- Exploration of non-equilibrium quantum dynamics in systems with >50 qubits
- Experiments with planar ion crystals with single-ion control

J. I. Cirac, P. Zoller, "Goals and opportunities in quantum simulation",
Nat. Phys. 8, 264 (2012)

R. Blatt, C. F. Roos, "Quantum simulations with trapped ions", Nat. Phys. 8, 277 (2012)

C. Monroe et al., "Programmable quantum simulations of spin systems with trapped ions"
Rev. Mod. Phys. 93, 025001 (2021)

Acknowledgements



Christine
Maier



Tiffany
Brydges



Florian
Kranzl



Manoj
Joshi



Helene
Hainzer



Dominik
Kiesenhofer



Tuomas
Ollikainen



Matthias
Bock

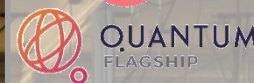


Johannes
Franke



Lukas
Pernthaler

Funding:



In collaboration with:

A. Elben,	}	Theory (Innsbruck)
B. Vermersch		
C. Kokail		
R. van Bijnen		
P. Zoller		
A. Schuckert	}	Theory (Munich)
I. Lovas		
M. Knap		
B. Lanyon	}	Experiment
R. Blatt		